



Chapter 7

EXTREME ULTRAVIOLET AND SOFT X-RAY LASERS

Hot dense plasma
lasing medium

Visible laser pump

λ

d

θ

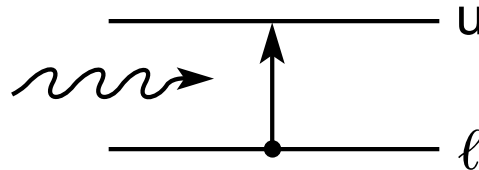
λ

$$\frac{I}{I_0} = e^{GL} \quad (7.2)$$
$$G = n_u \sigma_{\text{stim}} F \quad (7.4)$$
$$\sigma_{\text{stim}} = \frac{\pi \lambda r_e}{(\Delta\lambda/\lambda)} \left(\frac{g_l}{g_u} \right) f_{lu} \quad (7.18)$$
$$\frac{P}{A} = \frac{16\pi^2 c^2 \hbar (\Delta\lambda/\lambda) GL}{\lambda^4} \quad (7.22)$$

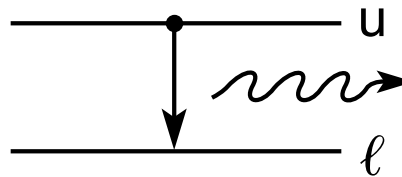


The Processes of Absorption, Spontaneous Emission, and Stimulated Emission

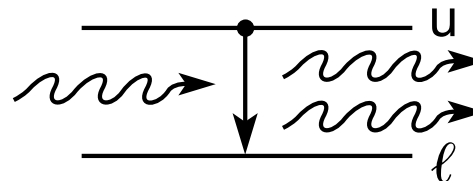
Absorption



Spontaneous emission

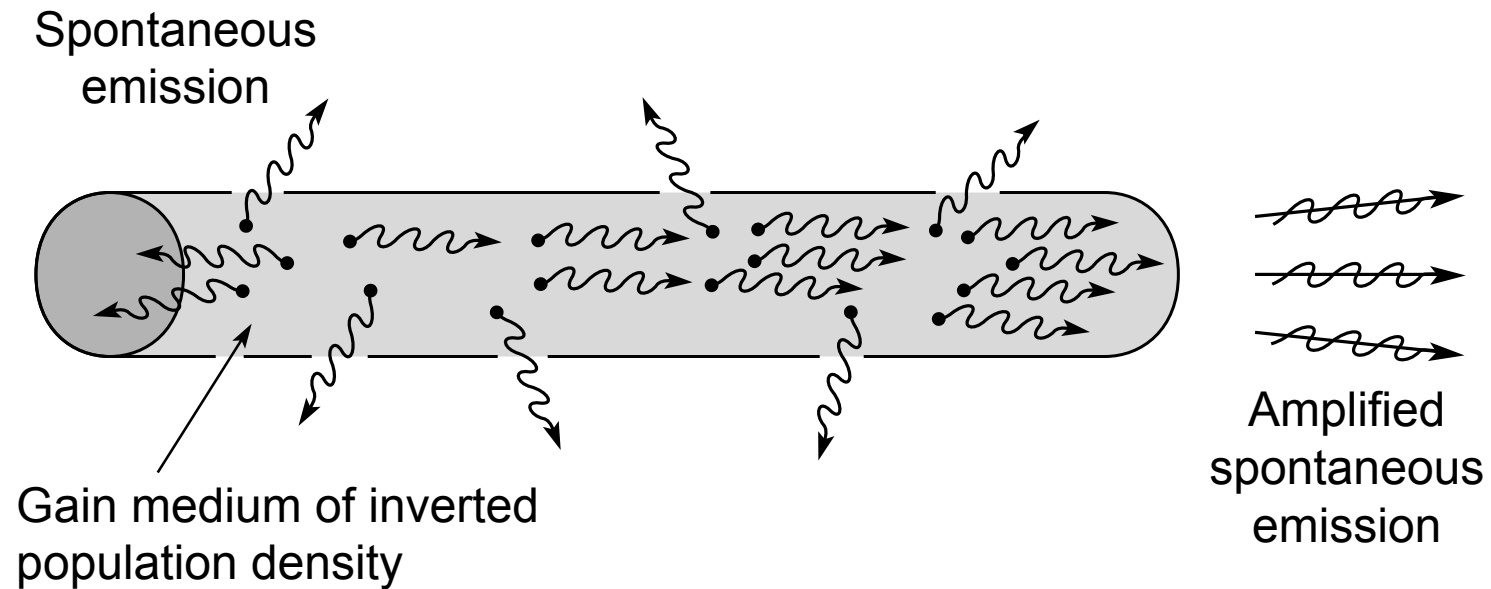


Stimulated emission





The Lasing Process Begins with Amplified Spontaneous Emission (ASE)

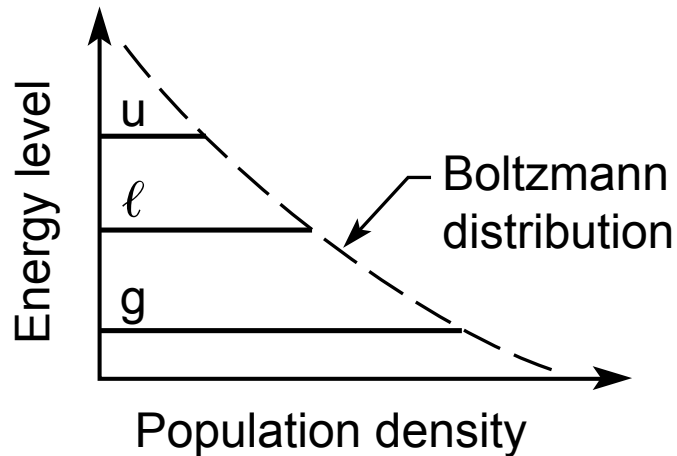


- both directions equally likely

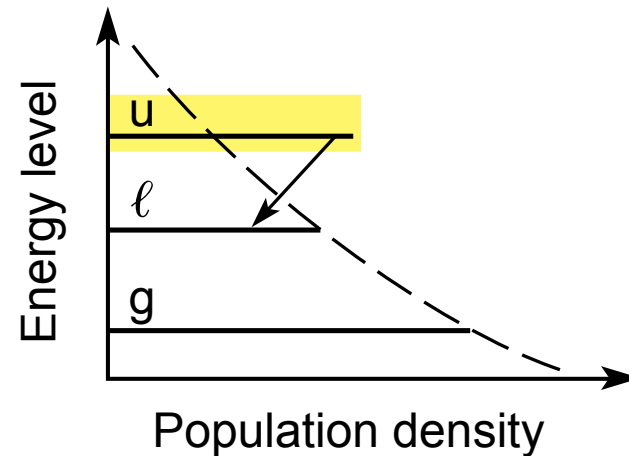


Equilibrium and Non-Equilibrium Energy Distribution

Equilibrium energy distribution



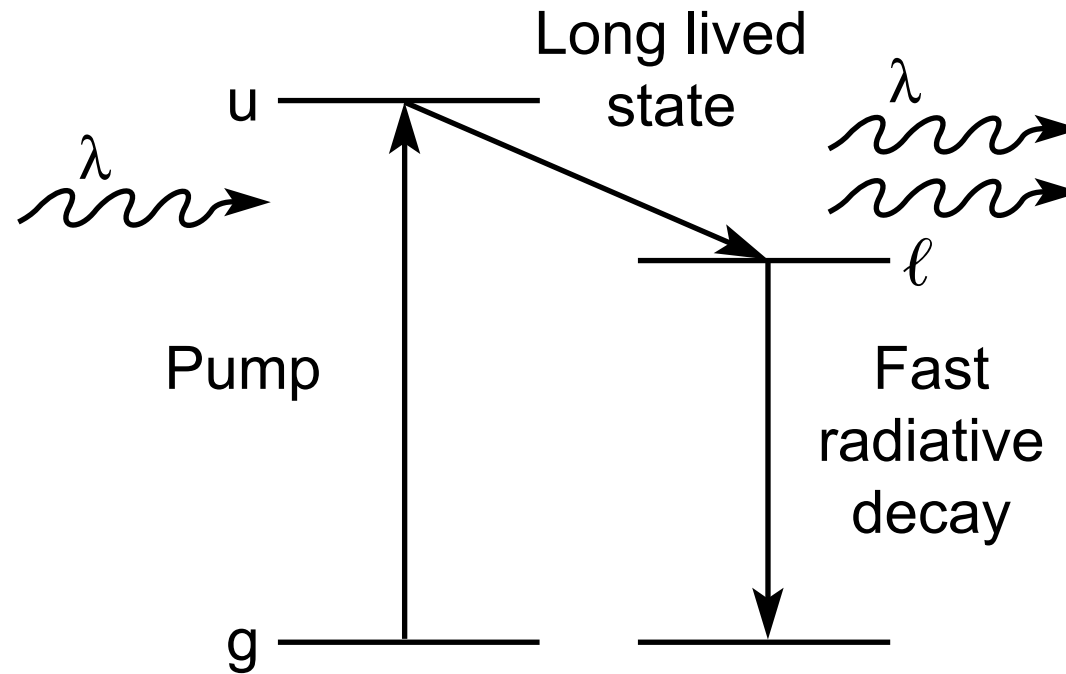
Non-equilibrium inverted energy distribution



Lasing requires an inverted population density (more atoms in the upper state than in the lower state).

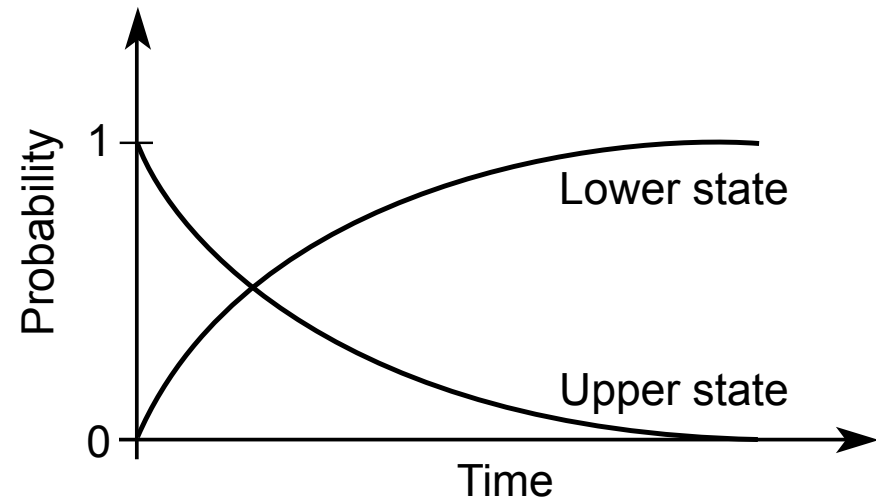
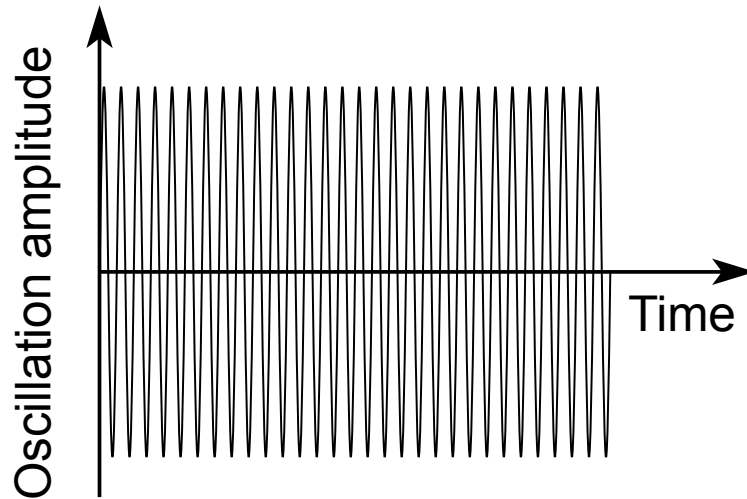


Three-level Lasing Between an Upper State u and a Lower State ℓ





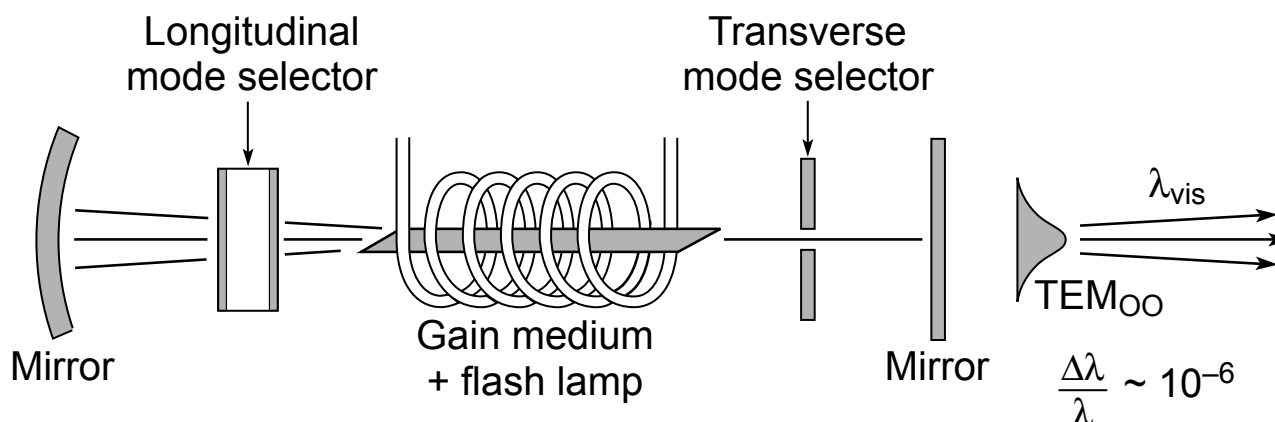
Radiative Decay Involves An Atom Oscillating Between Two Stationary States at the Frequency $\omega_{if} = (E_i - E_f) / \hbar$



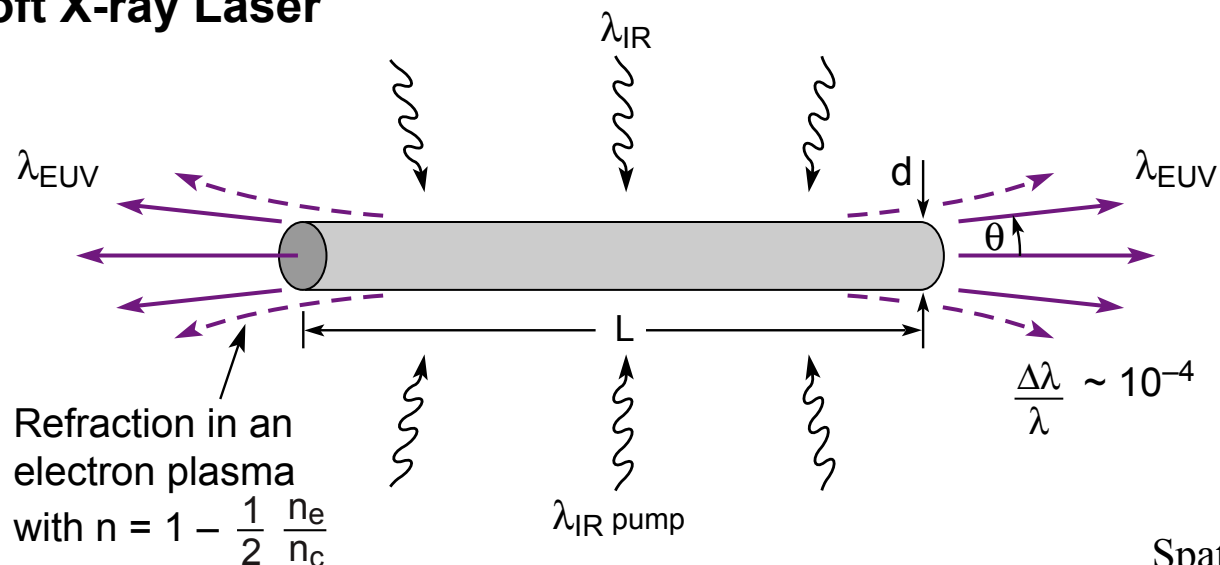


EUV/SXR Lasers are High Gain With Minimal Cavity Optics

Visible Light Laser



EUV/Soft X-ray Laser



Spatial and temporal coherence addressed in chapter 8.



Early Successes With Lasing in the 4-46 nm Wavelength Region

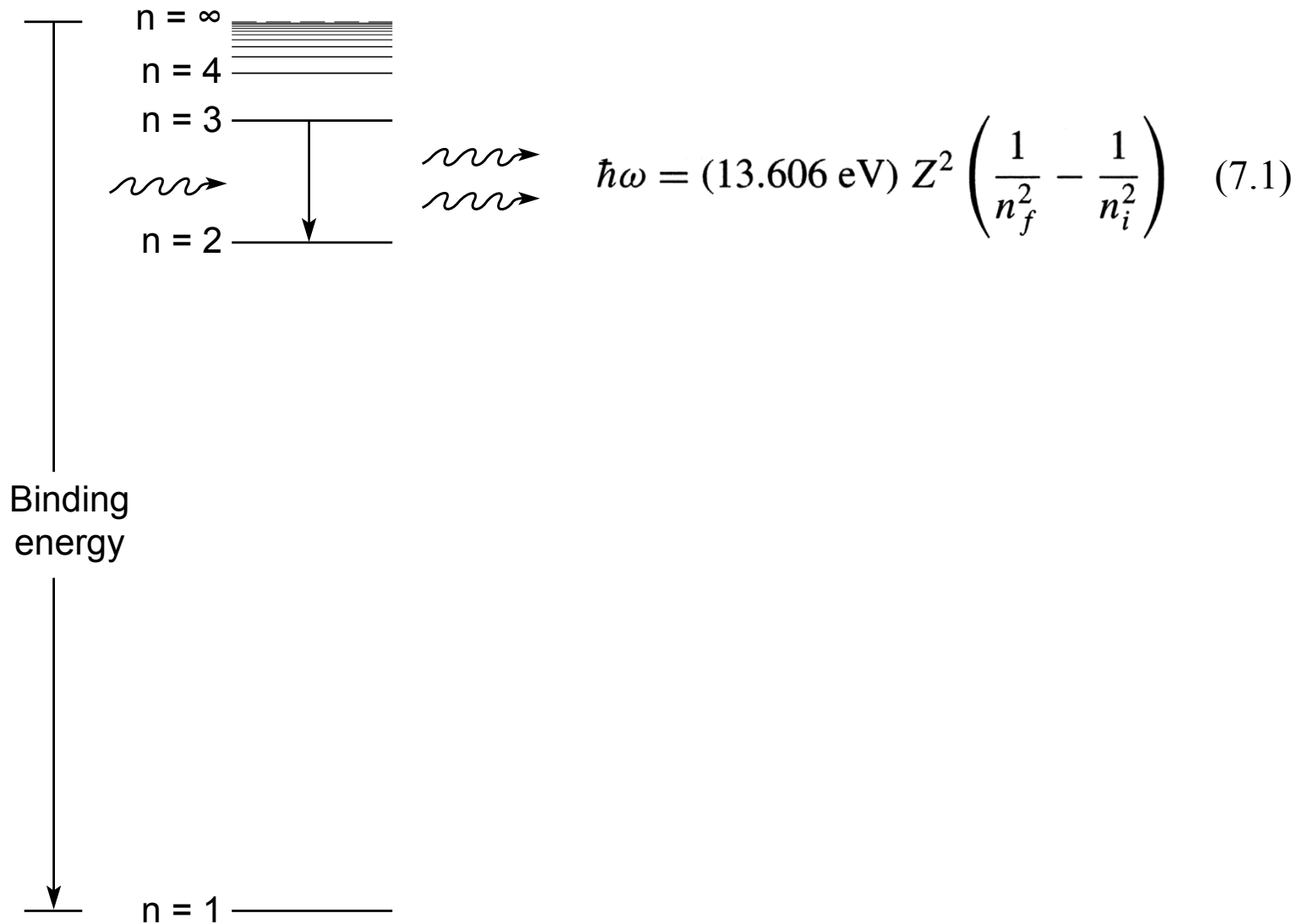
- **Recombination lasing in rapidly cooled H-like carbon**
- **Collisionally pumped lasing in Ne-like Se**
- **Extension to shorter wavelengths with collisionally pumped Ni-like Ta, W, . . .**
- **Saturation of Ni-like Ag, In, Sn, Sm, . . . with refraction compensated plasmas**

More recently:

- **Table-top lasing in the EUV with high spatial coherence and mW average power**
- **Compact lasing with f_{sec} transient gain techniques**



Stimulated $n = 3$ to $n = 2$ Emission for a Hydrogen-Like Ion





Transitions in Single Electron, Hydrogen-Like Carbon Ions ($Z = 6$)

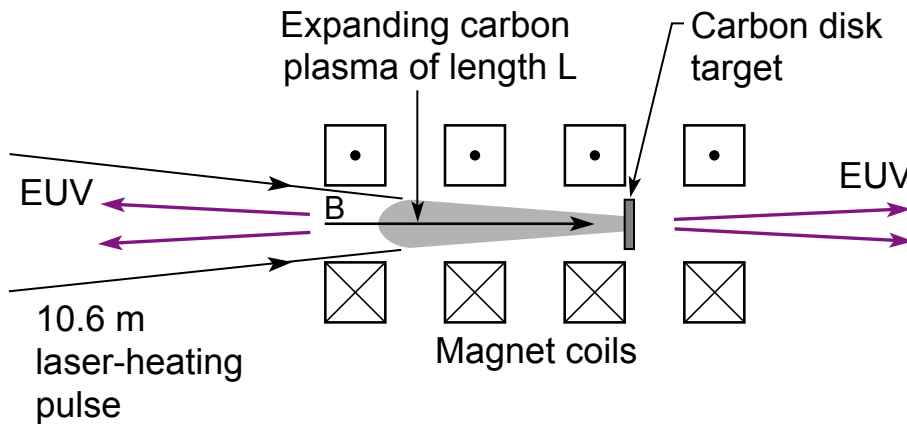
$$\hbar\omega = (13.606 \text{ eV}) Z^2 \left(\frac{1}{n_f^2} - \frac{1}{n_i^2} \right) \quad (7.1)$$

Transition $u-l$	Photon energy $\hbar\omega$ (eV)	Wavelength λ (nm)	Oscillator strength ^a f_{lu}	Lifetime $\tau = 1/A_{ul}$ (ps)
2p-1s	367.0	3.378	0.4162	1.2
3p-1s	435.0	3.350	0.0791	
4p-1s	458.7	2.703	0.0290	
3p-2s	68.03	18.22	0.435	4.1
3s-2p	68.03	18.22	0.0136	
3d-2p	68.03	18.22	0.696	12.0
4p-2s	91.84	13.50	0.103	
4s-2p	91.84	13.50	0.0030	
4d-2p	91.84	13.50	0.122	
4p-3s	23.81	52.07	0.485	

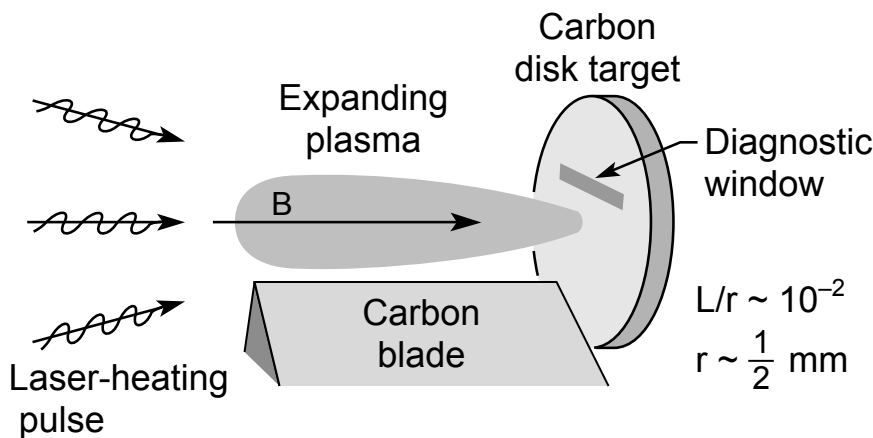
- $\hbar\omega \propto Z^2$
- $\tau \propto \tau_H/Z^4$



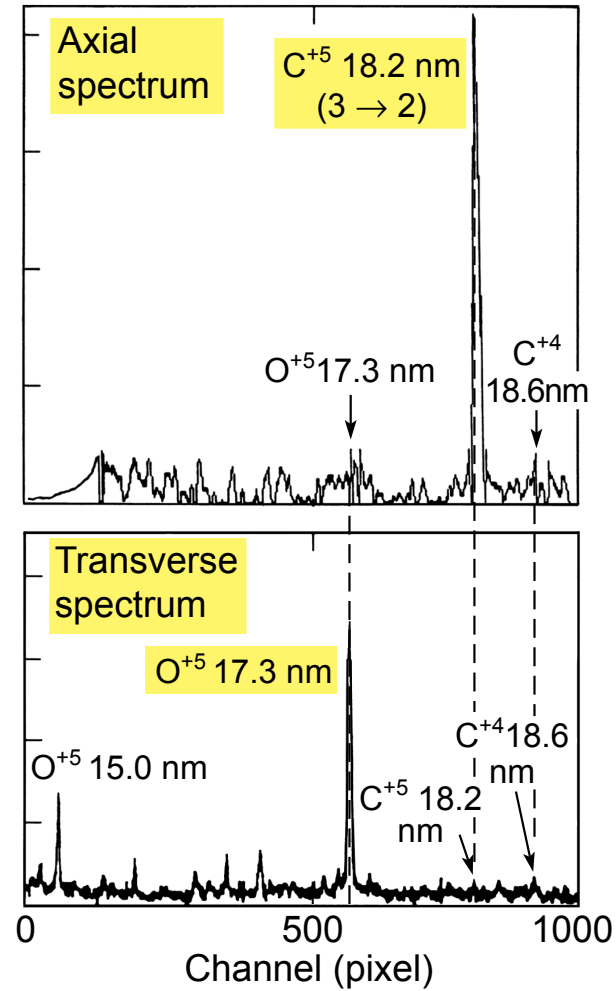
Recombination Lasing With H-like Carbon Ions



CO₂ laser: 10.6 μm , 5×10^{12} W/cm², 70 ns
 Ionization of C⁺⁵ = 490 eV
 Plasma: $\kappa T = 100\text{-}200$ eV, 5×10^{18} e/cm³



Recombination of C⁺⁶ and e⁻ cascading down excitation states (n)



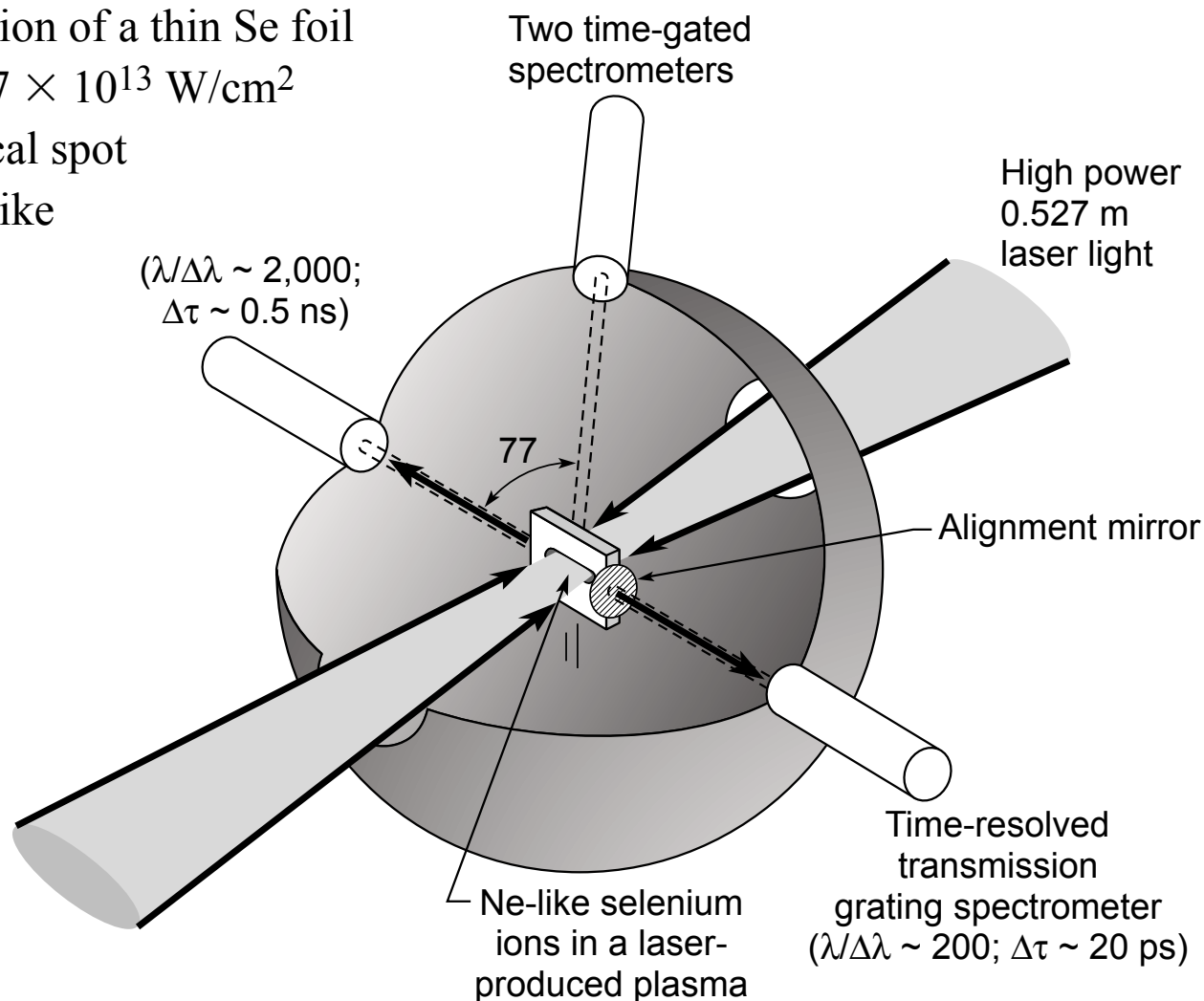
Courtesy of S. Suckewer et al. (1985) Princeton University



Laser Produced Plasma for Ne-like Lasing in Selenium ($Z = 34$)



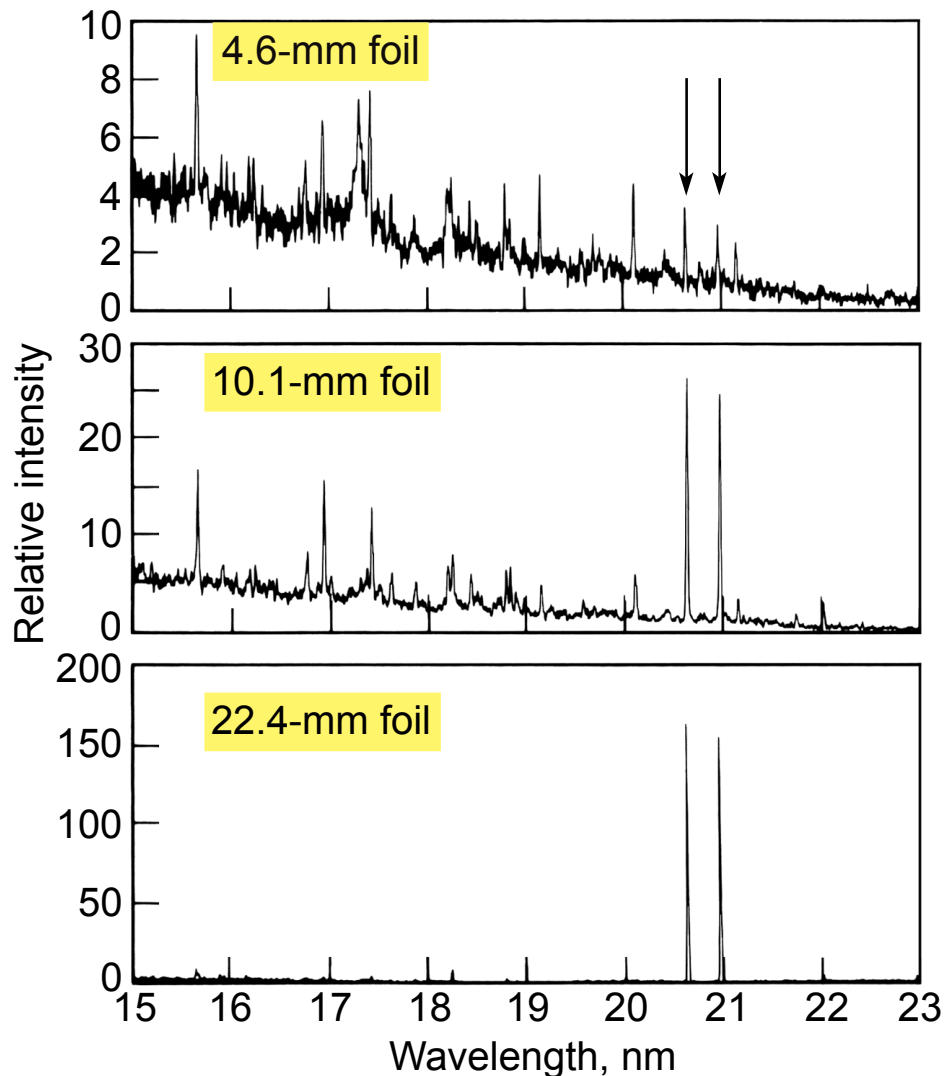
- Double-sided irradiation of a thin Se foil
- 2.4 TW, 2ω , 450 ps, 7×10^{13} W/cm²
- 200 $\mu\text{m} \times 1.1$ cm focal spot
- About 20% ions Ne-like
- Ionization of F1-like Se^{+23} is 1036 eV (Ne-like is 2540 eV)



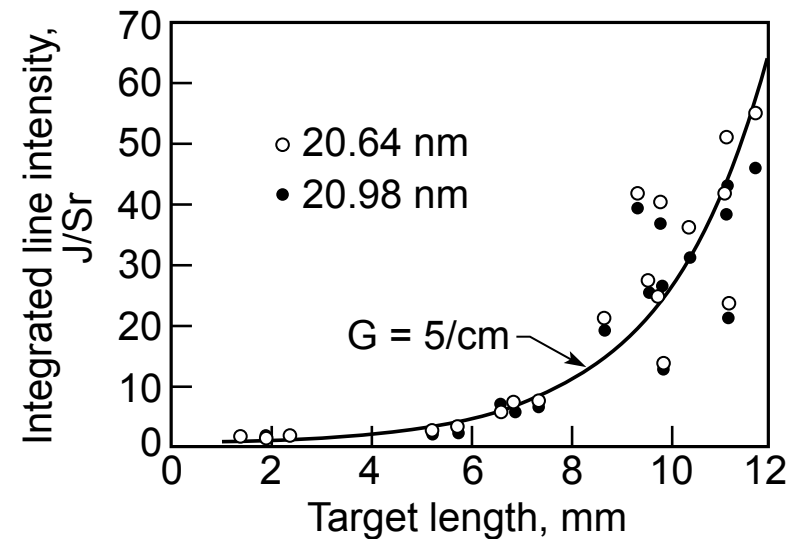
Courtesy of D. Matthews et al. (1985)
Lawrence Livermore National Laboratory



Exponential Gain Observed With Increasing Plasma Length



- Gain in axial direction only
- Use of on and off-axis time gated spectrometers
- $3p \rightarrow 3s$ lasing at 20.64 nm and 20.98 nm in Ne-like Se^{+24}

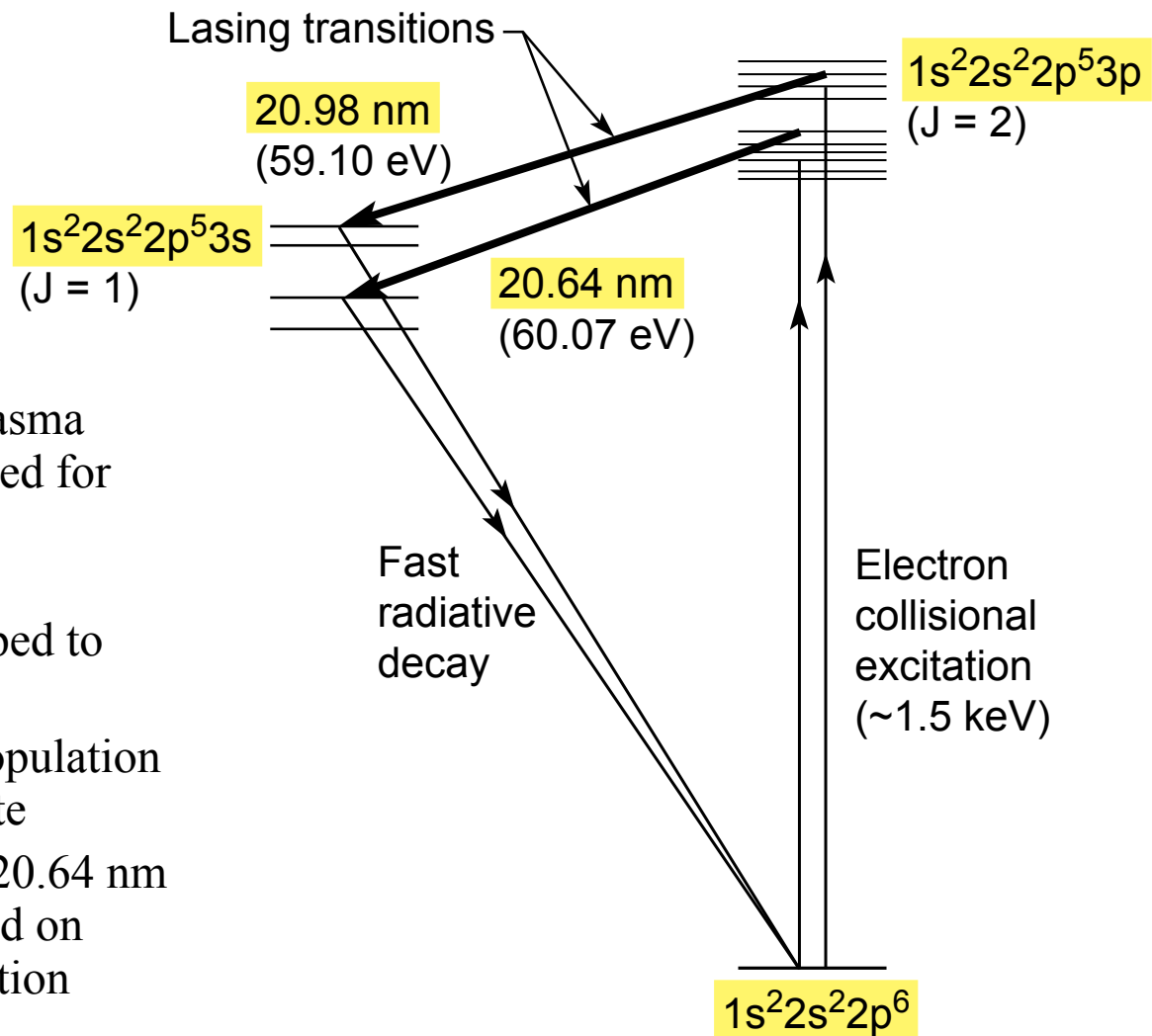


Courtesy of D. Matthews et al. (LLNL)

Population Inversion in Neon-like Selenium



Simplified Energy Level Diagram for Se^{+24}



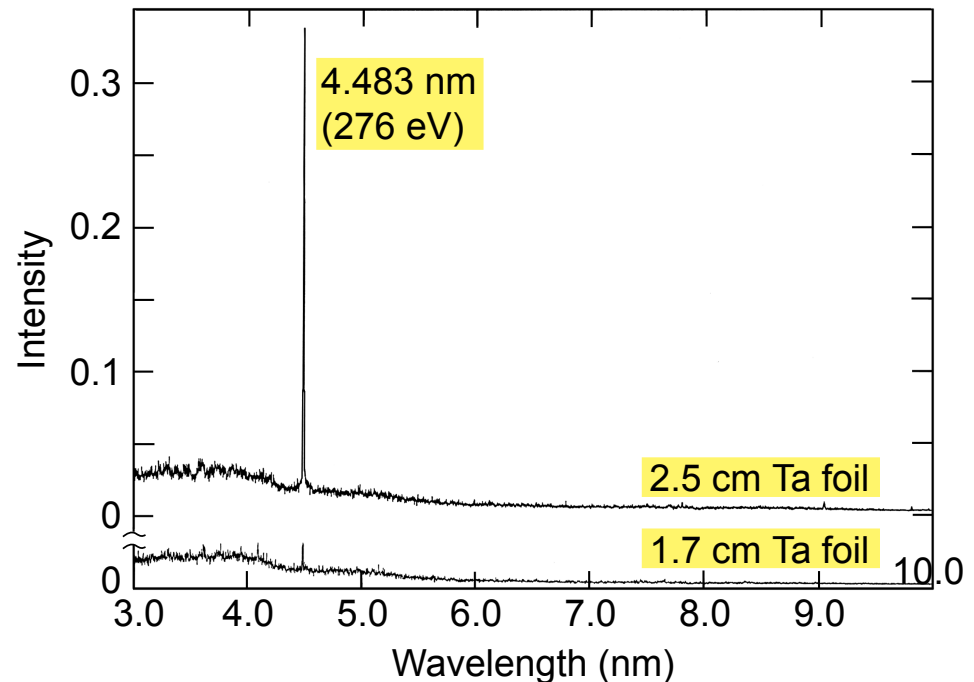
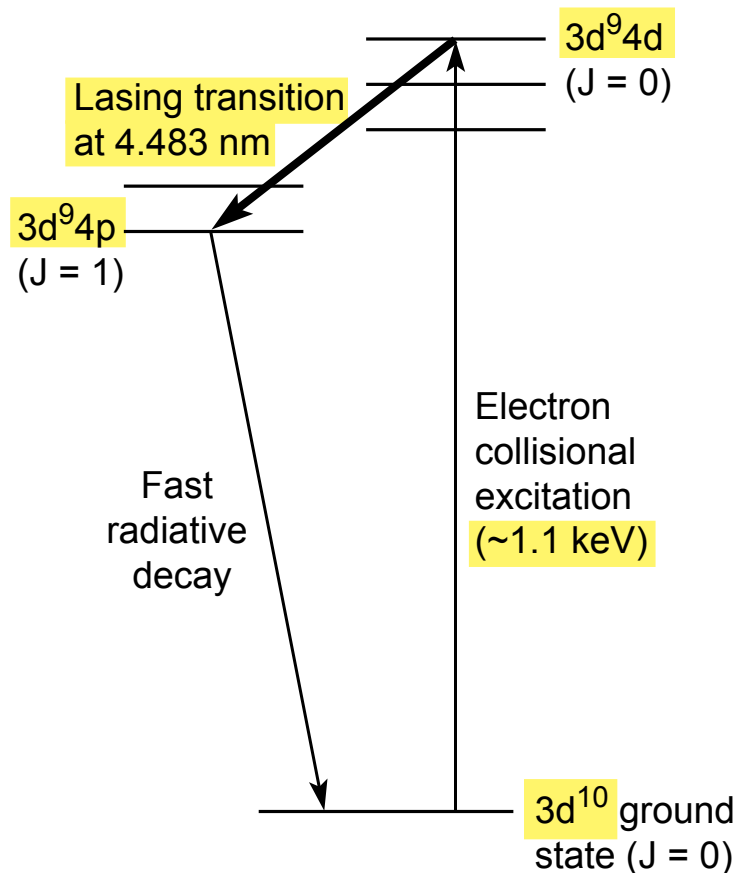
- Laser produced plasma conditions optimized for dominant Ne-like ionization stage
- Collisionally pumped to a 3p excited state
- Fast radiative depopulation of the lower 3s state
- $3p \rightarrow 3s$ lasing at 20.64 nm and 20.98 nm based on selective depopulation

Courtesy of M. Rosen et al. (1985), LLNL.

Extension to Nickel-like Ions Permits Lasing at Shorter Wavelengths Without the Need for Higher Electron Temperature



Lasing in Ni-like Ta⁺⁴⁵

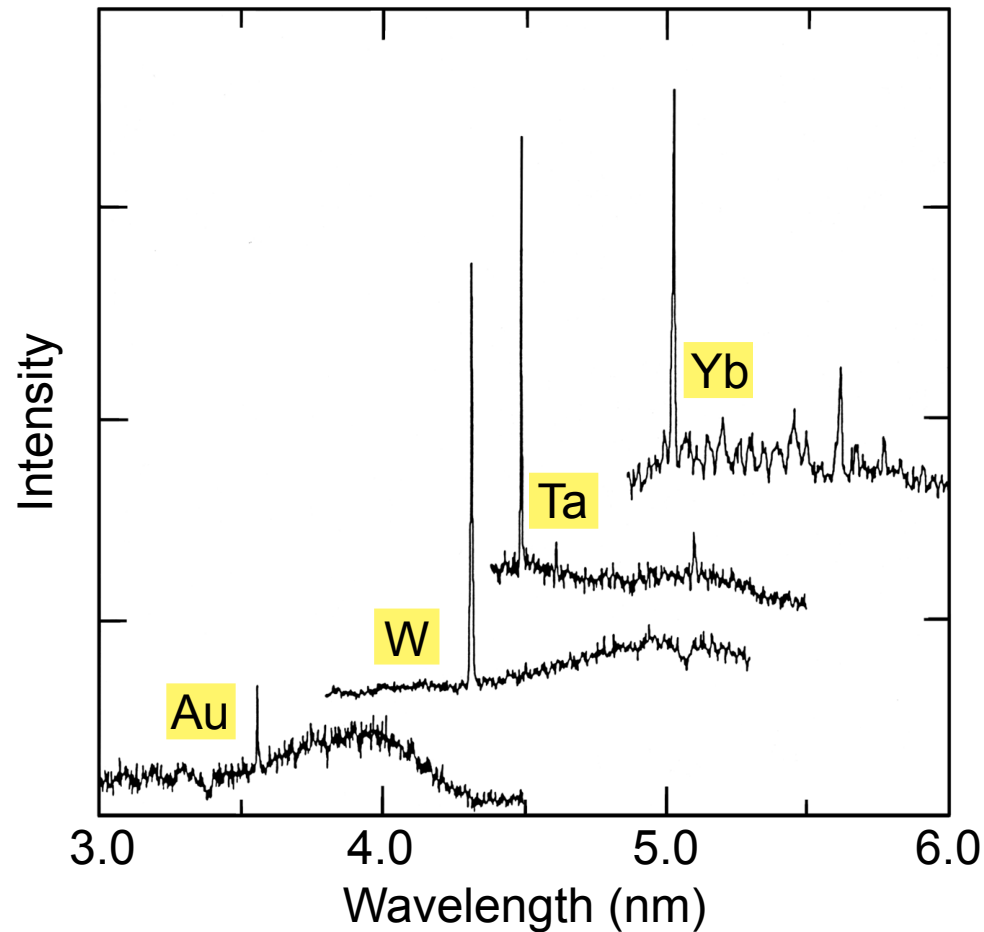


Courtesy of B. MacGowen et al. (1987), LLNL.

- Ni-like Ta ($Z = 73$, $28 e^-$, $+45$)
- $1s^2 2s^2 2p^6 3s^2 3p^6 3d^{10}$ ground state ($28 e^-$)



Nickel-like Lasing Across the K-edge of Neutral Carbon



4d → 4p lasing

- W at 4.318 nm
- Ta at 4.483 nm
- C-K at 4.36 nm

The water window is defined by the K-absorption edges of neutral carbon and oxygen.

Courtesy of B. MacGowen et al. (1987), LLNL.



Refractive Index of a Plasma

For $\omega > \omega_p$ there is a real propagating wave with phase velocity

$$v_\phi = \frac{\omega}{k} = \frac{c}{\sqrt{1 - \omega_p^2/\omega^2}} = \frac{c}{\sqrt{1 - n_e/n_c}} \quad (6.113a)$$

The refractive index of the plasma is

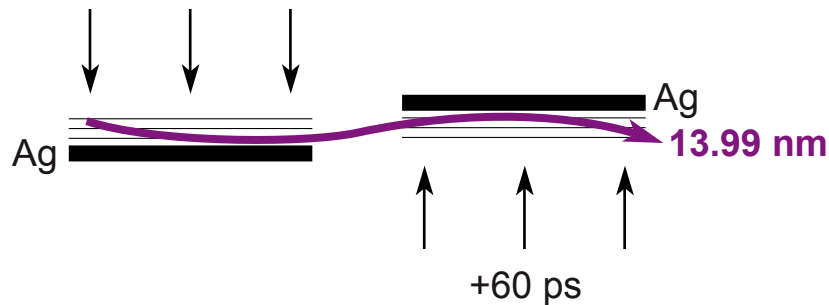
$$n = \sqrt{1 - \frac{\omega_p^2}{\omega^2}} \quad (6.114a)$$

or equivalently

$$n = \sqrt{1 - \frac{n_e}{n_c}} \quad (6.114b)$$



Refraction Compensating Double-Targets Used to Achieve Saturation of Lasing at 13.99 nm in Ni-like Ag



Nd laser: $1.05 \mu\text{m}$, $2 \times 10^{13} \text{ W/cm}^2$, 75 ps

Target: Ag stripes, $200 \mu\text{m} \times 25 \text{ mm}$

Plasma: 700 eV , $6 \times 10^{20} \text{ e/cm}^3$
 $43 \times 57 \mu\text{m}$, $1.5 \times 3.5 \text{ mrad}$

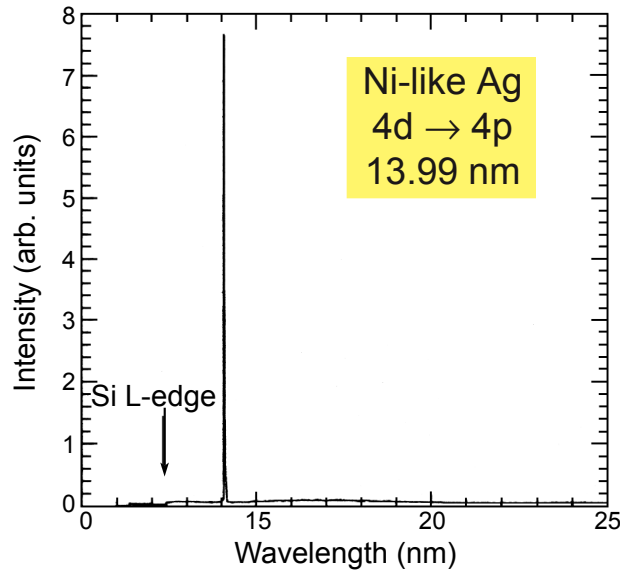
- Prepulse allows plasma expansion, decreases transverse electron density gradients and increases plasma volume
- Double targets permit refraction compensation (opposite turning angles) and double the gain length.
- Time delay of one target irradiation enhances gain in one direction
- Saturated $4d \rightarrow 4p$ lasing at 13.99 nm in Ni-like Ag^{+19} ($Z = 47$, $28e^-$)

Courtesy of J. Zhang et al. (1997)
Rutherford Appleton Laboratory



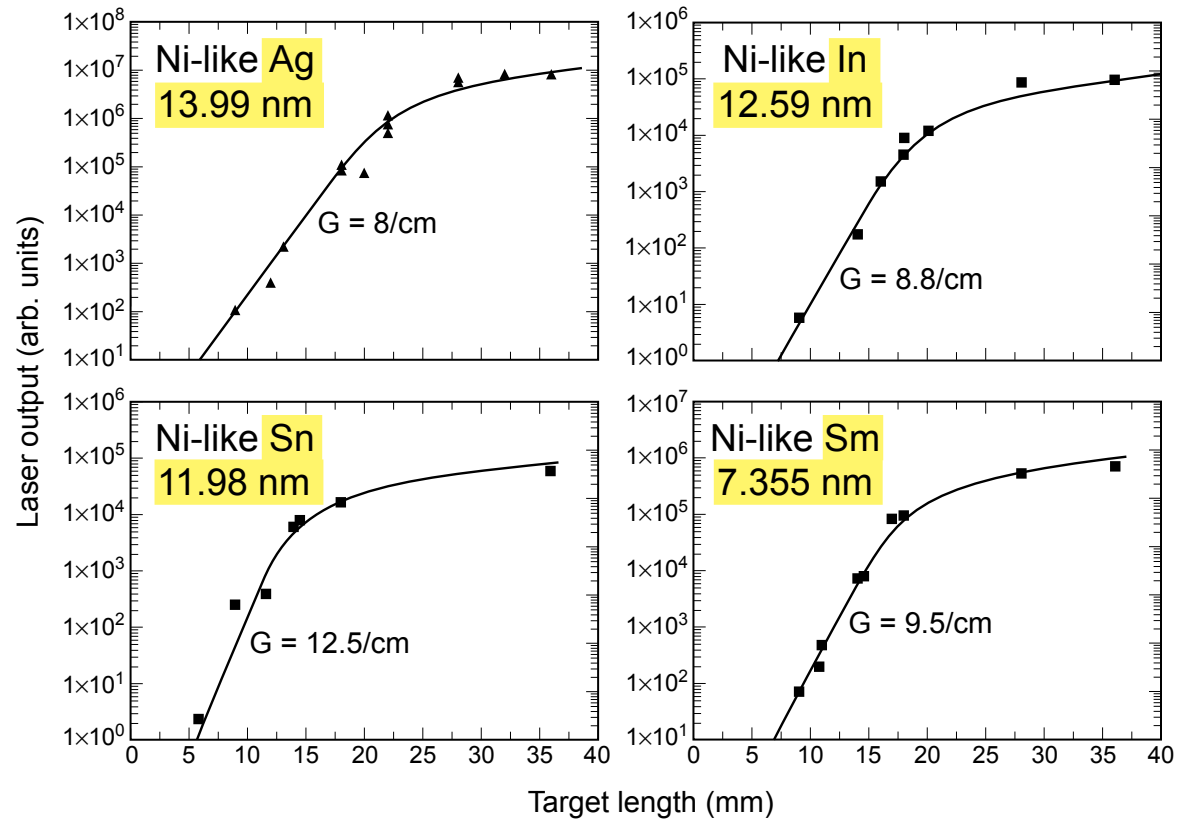
Saturation of Nickel-like Lasing in Ag, In, Sn, and Sm

Refraction compensating double targets



Courtesy of J. Zhang et al. (1977)
Appleton Rutherford Laboratory

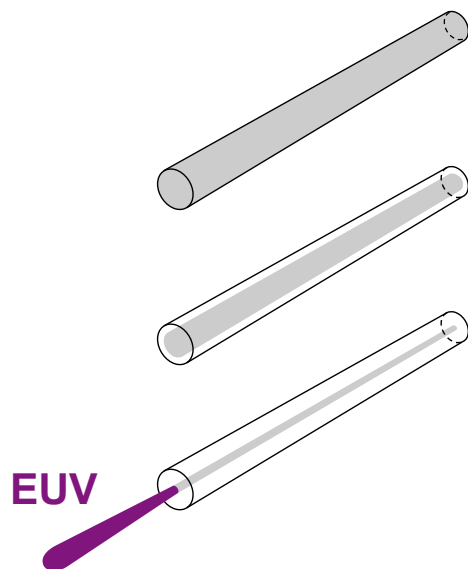
Note: Wavelengths quoted are calculated by J. Scofield and B. MacGowan



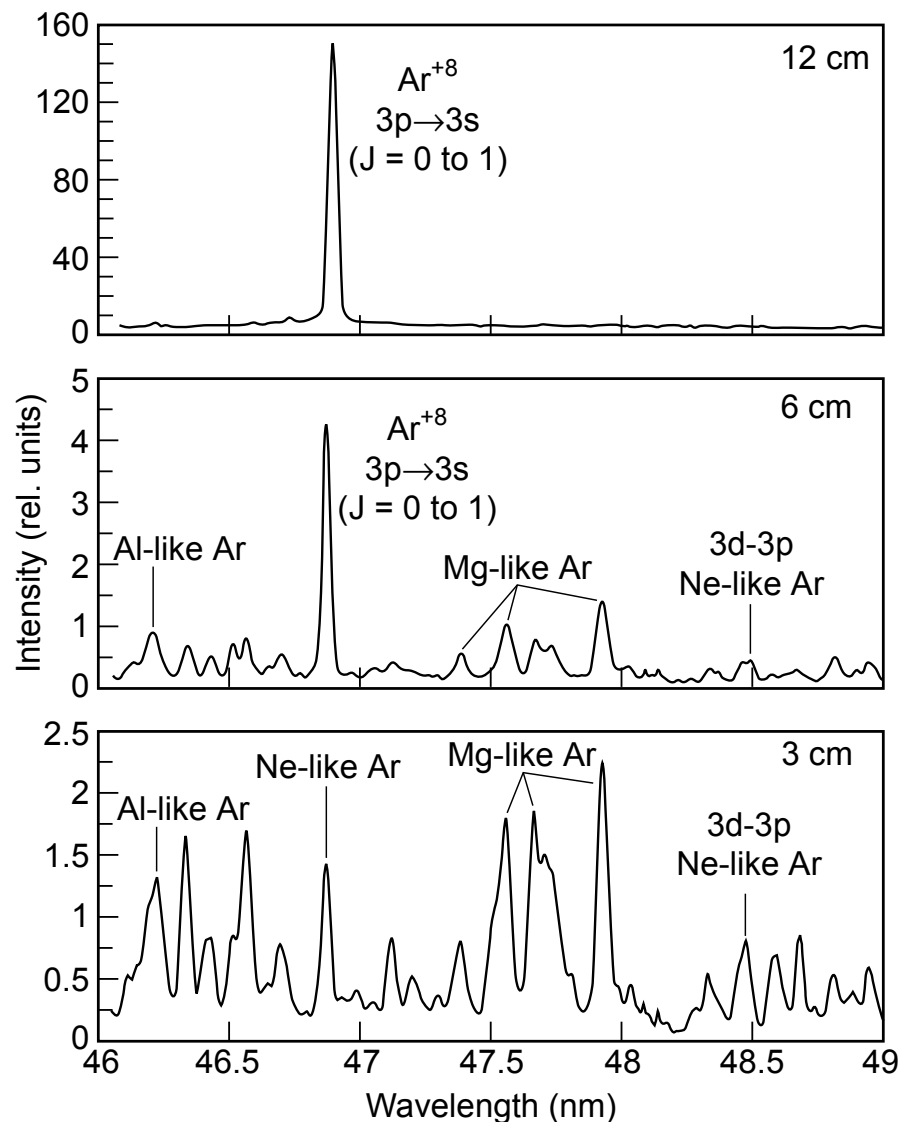
Courtesy of J.Y. Lin et al. (1999)
Appleton Rutherford Laboratory



High Average Power, High Spatial Coherence Table-Top Laser at 46.86 nm



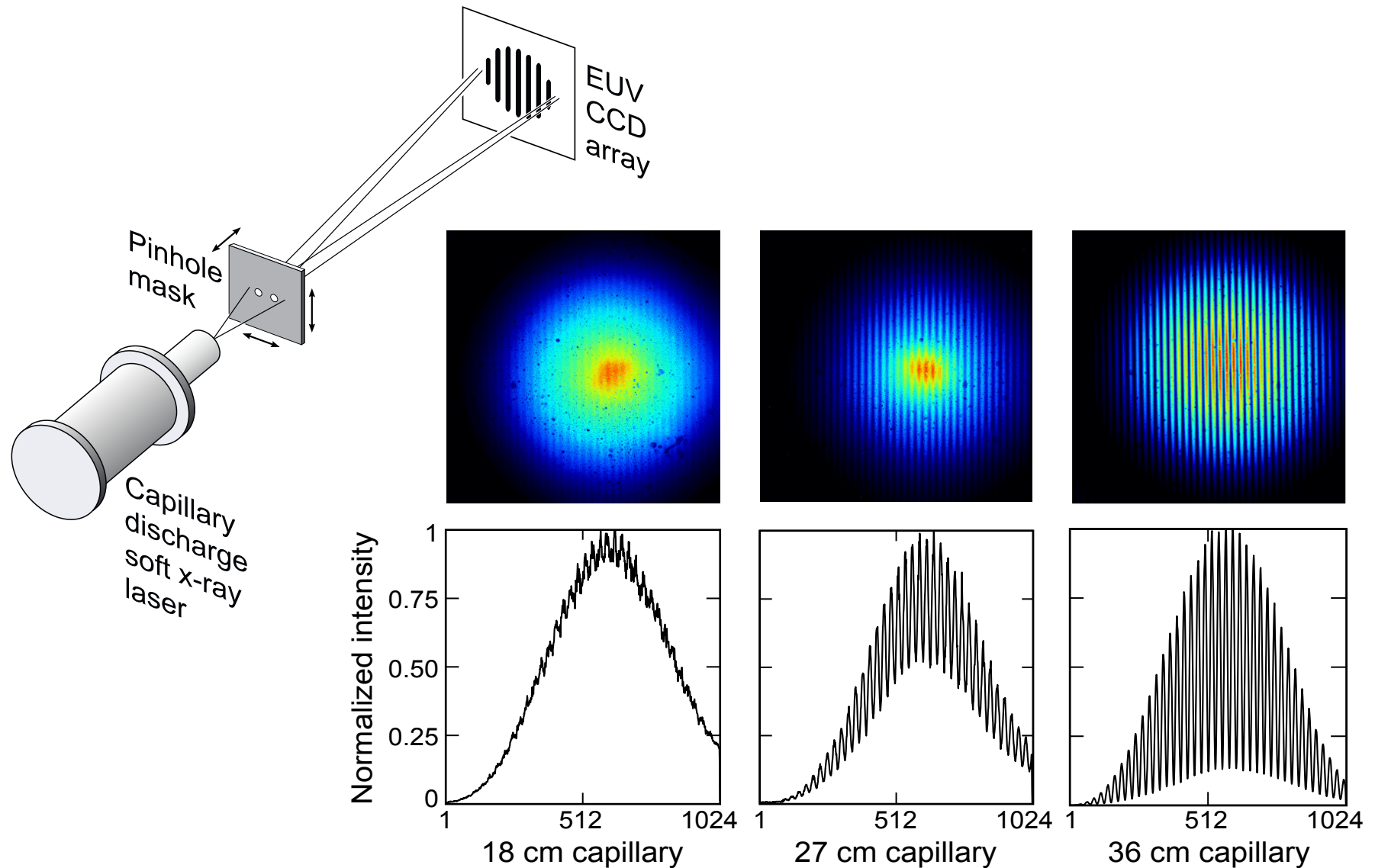
- Discharge plasma
- Fast, high current pulse compresses ($\mathbf{J} \times \mathbf{B}$) and heats plasma
- 70 eV, $5 \times 10^{18} \text{ e/cm}^3$
 $300 \mu\text{m}^D \times 36 \text{ cm long (1:1000)}$
- Ne-like Ar^{+8} , $3p \rightarrow 3s$ at 46.86 nm
- $\bar{P} = 3.5 \text{ mW}$, spatially coherent



Courtesy of J. Rocca (1995), Colorado State University



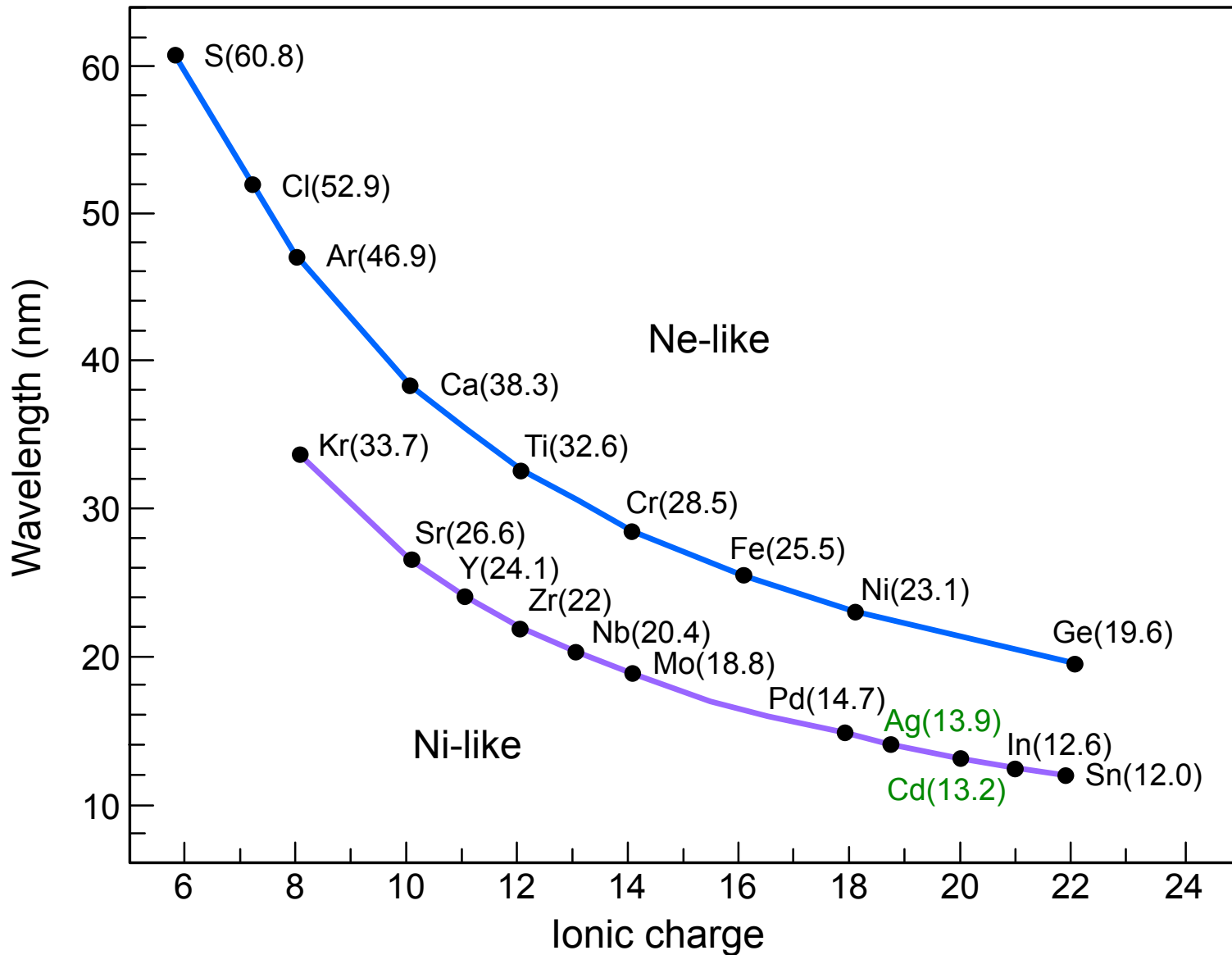
Spatial Coherence of 46.86 nm Laser



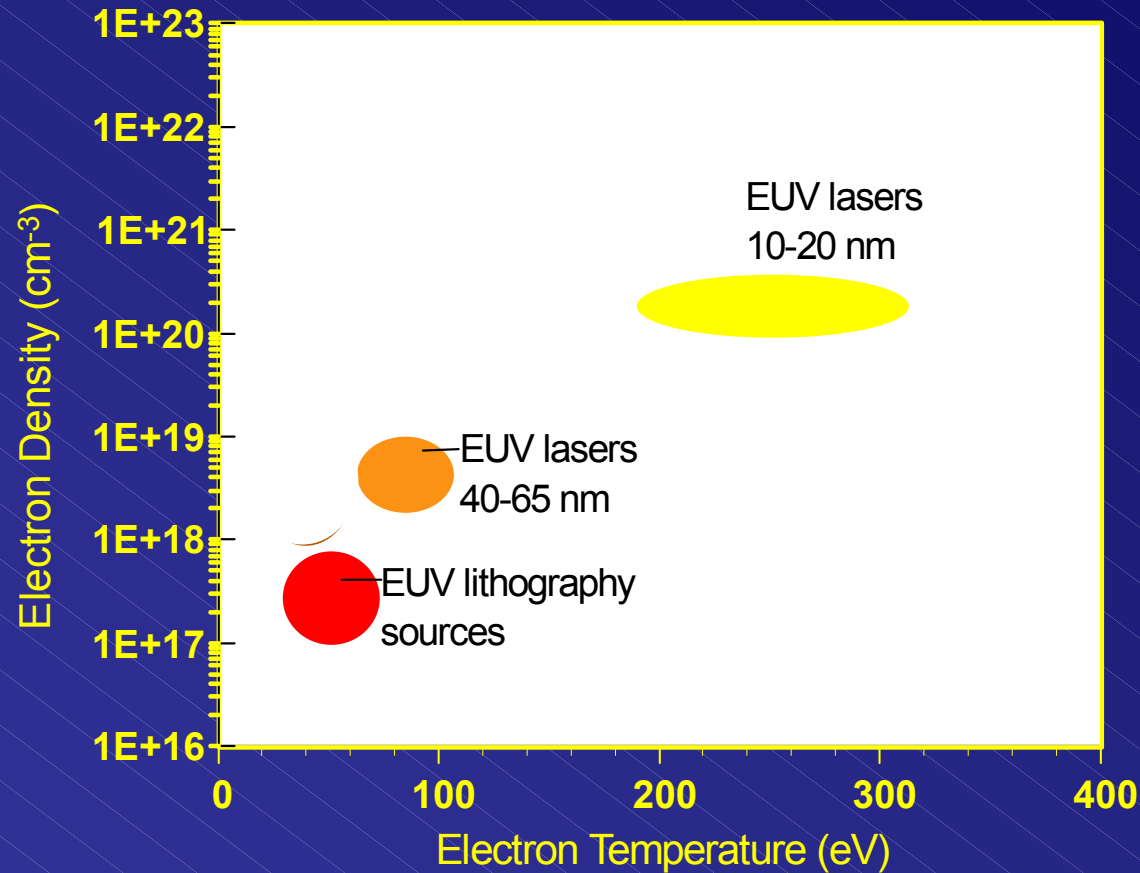
Courtesy of Y. Liu, UC Berkeley, and J. Rocca, Colorado State University (2001)



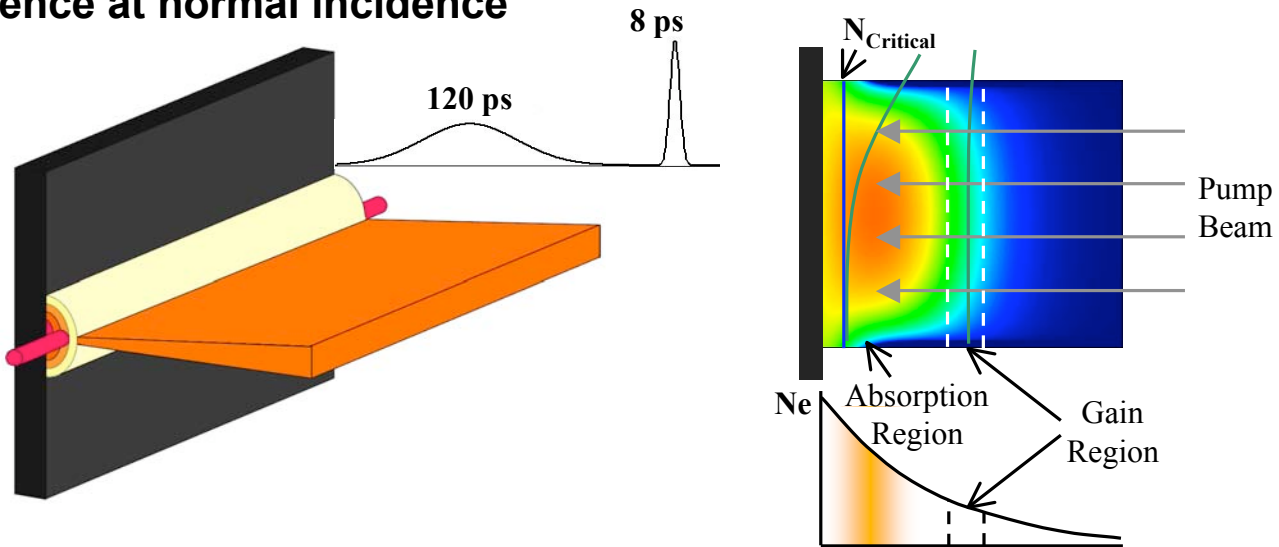
Scaling to 13 nm Requires Excitation of Ni-Like Cd Ions (Cd + 20)



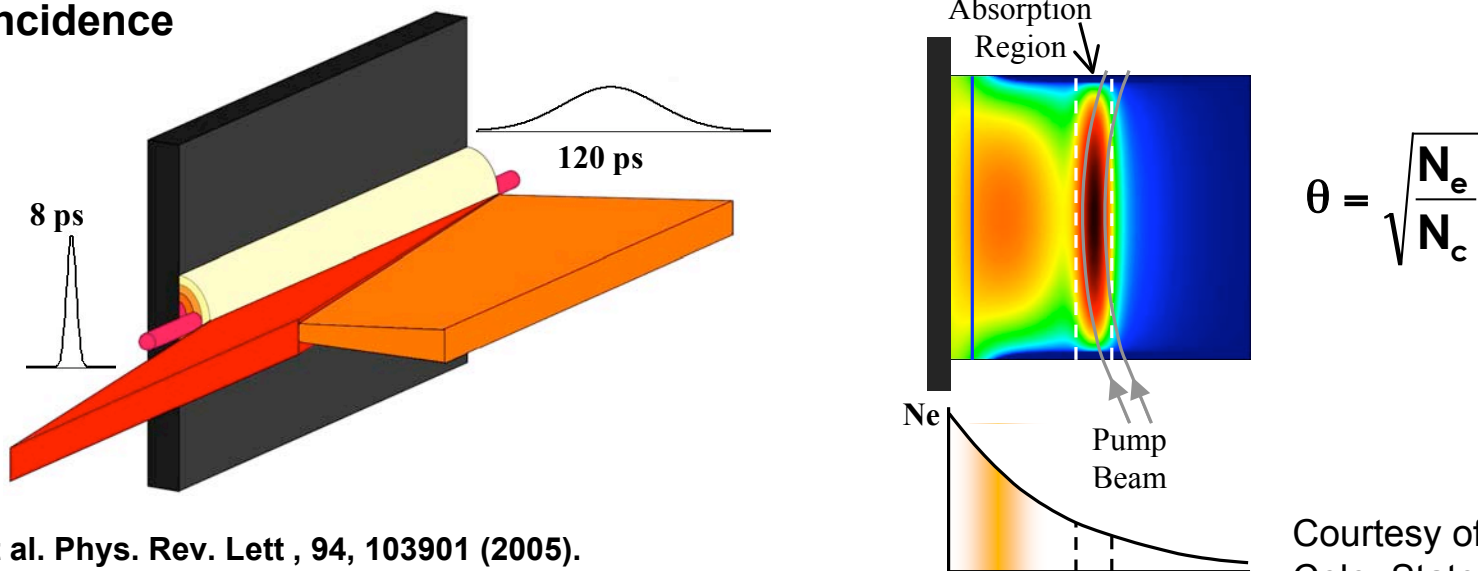
Generation of laser radiation at 13 nm requires significantly hotter and denser plasma columns



• Two pulse sequence at normal incidence



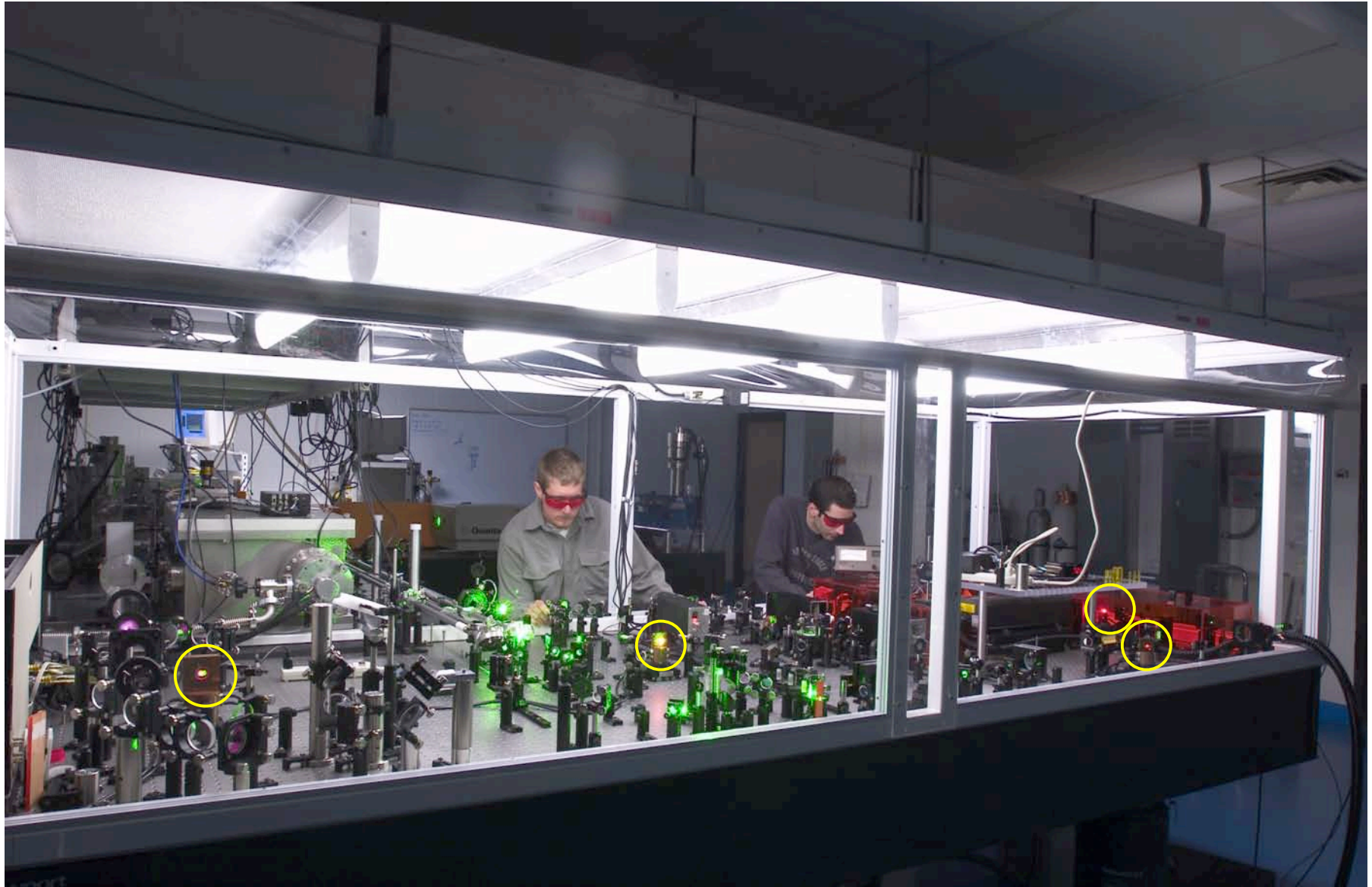
• Grazing incidence



* R. Keenan, et al. Phys. Rev. Lett, 94, 103901 (2005).
B.M. Luther et al. Optics Lett, 30, 165 (2005)

Courtesy of J. Rocca
Colo. State U.

5-10 Hz Pump laser: 1 J Short Pulse Table-top Ti:Sapphire System

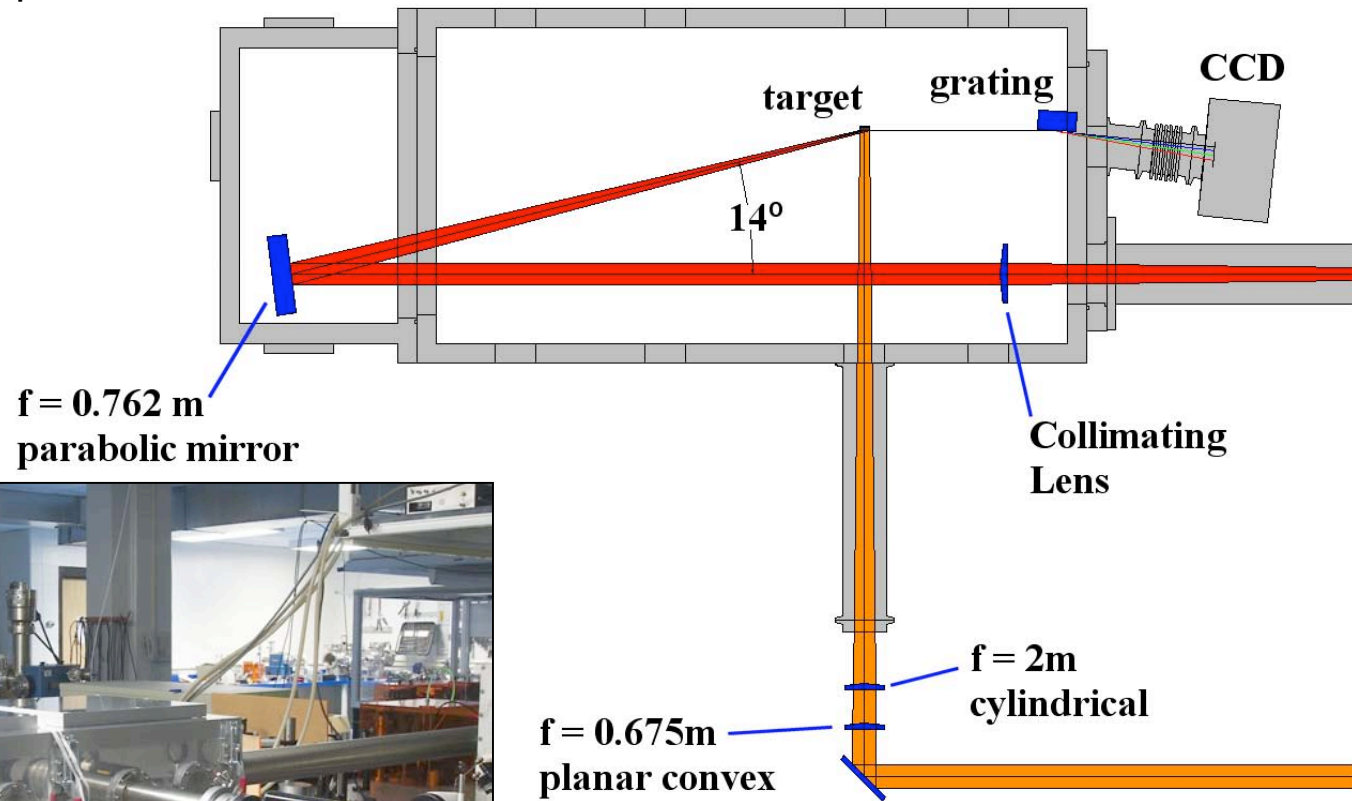


Courtesy of J. Rocca, Colo. State U.

Configuration for 30 μm wide short pulse line focus at 14 to 26 degrees grazing incidence

Line Focus

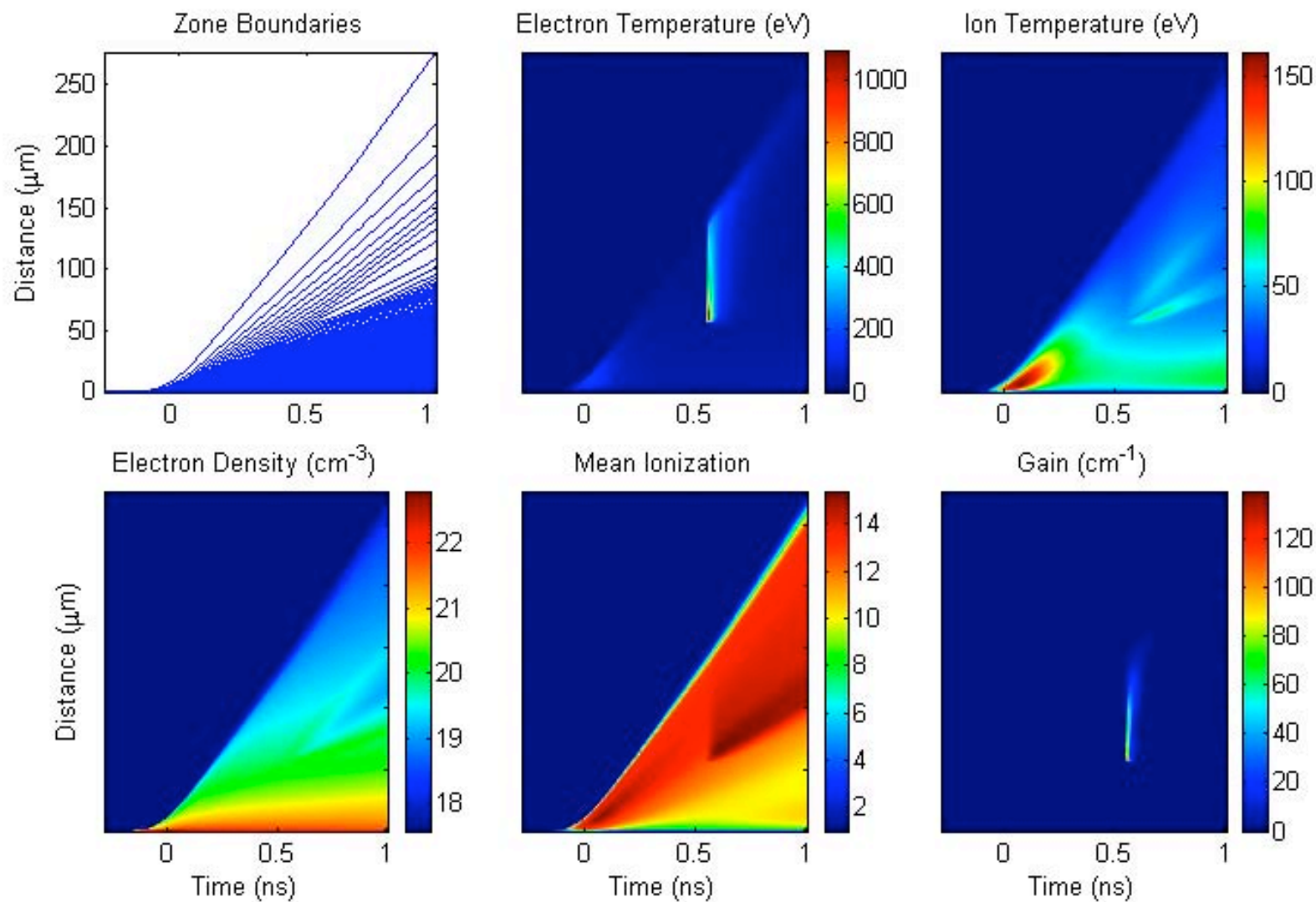
- Pre-pulse: 30 μm FWHM,
- Short-pulse: 30 μm FWHM,



Courtesy of J. Rocca, Colo. State U.

Simulation predicts high gain at 18.9 nm in Ni-like Mo, $g \sim 100 \text{ cm}^{-1}$ (Mark Berrill, CSU)

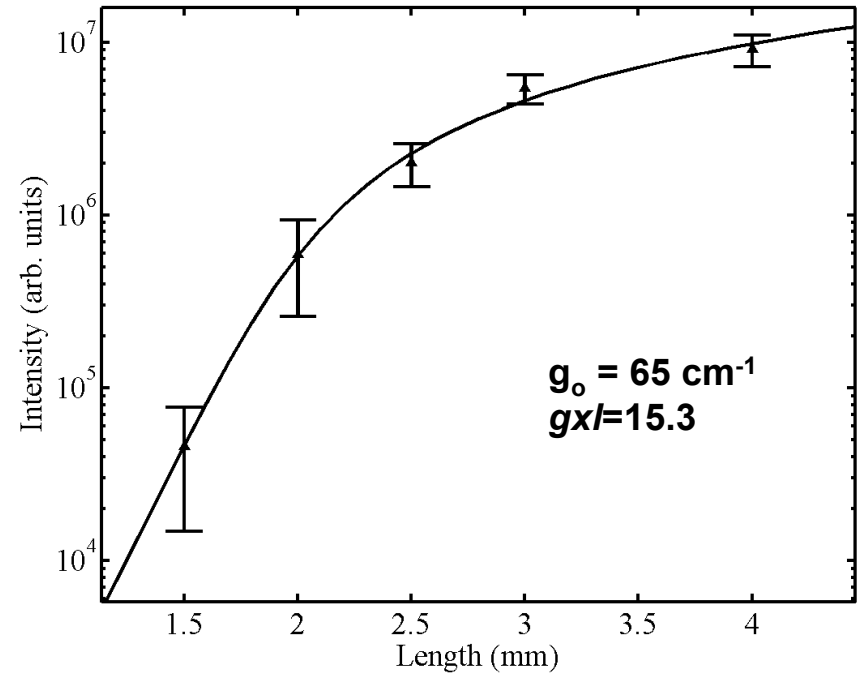
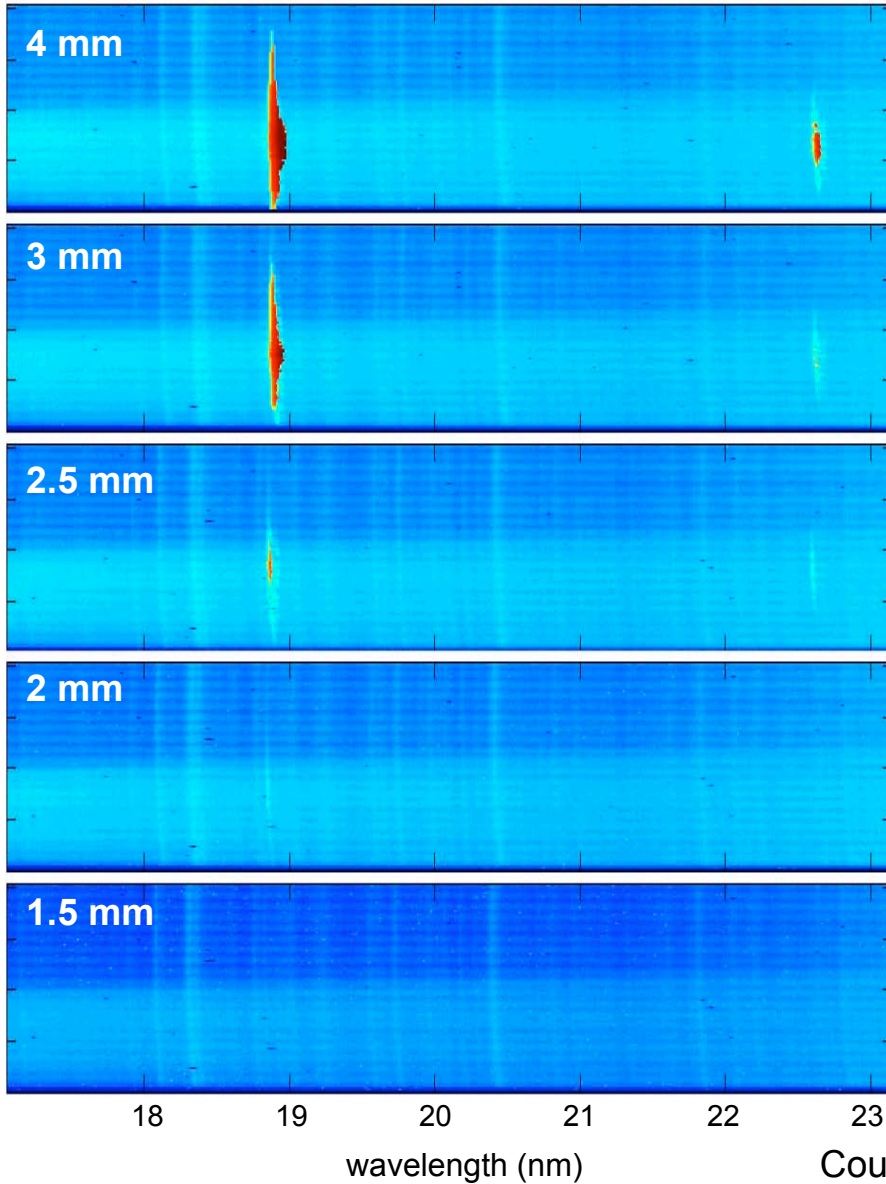
Pre-pulse: 330 mJ, 120 ps Heating pulse: 800 mJ, 8 ps heating pulse



Courtesy of J. Rocca, Colo. State U.

Saturated 18.9 nm Ni-like Molybdenum Laser

Long pulse: 340 mJ - Short pulse: 1 J



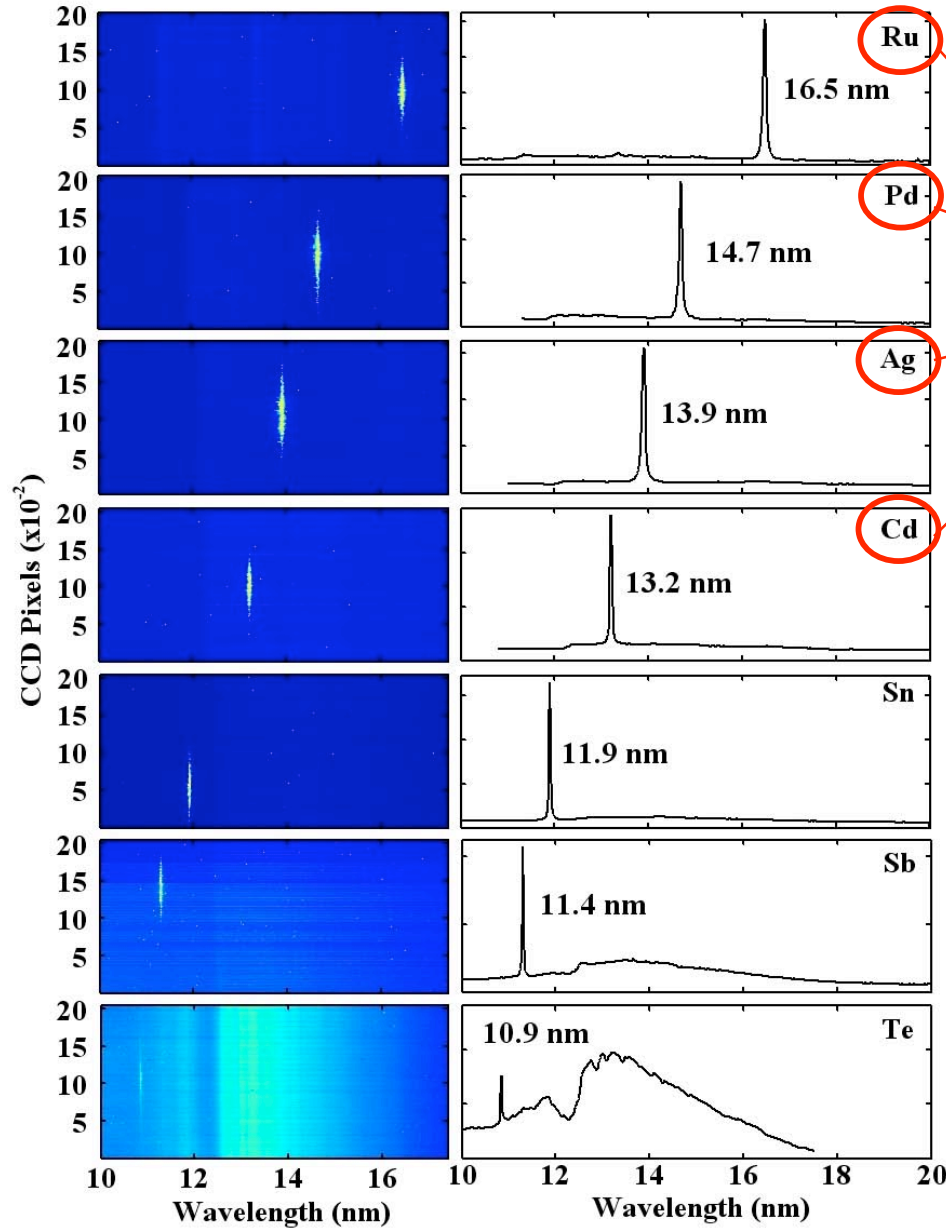
Fit with the expression from Tallents et. al.
8th Int. Conf. XRL, AIP Vol. 641, 2002.

$$GL + 2 \frac{I_{av}}{I_s} = g_0 L$$

$$I_{av} = I_0 \frac{[\exp(GL) - 1]^{3/2}}{[GL \exp(GL)]^{1/2}}$$

Courtesy of J. Rocca, Colo. State U.

Lasing observed at wavelengths as short as 10.9 nm

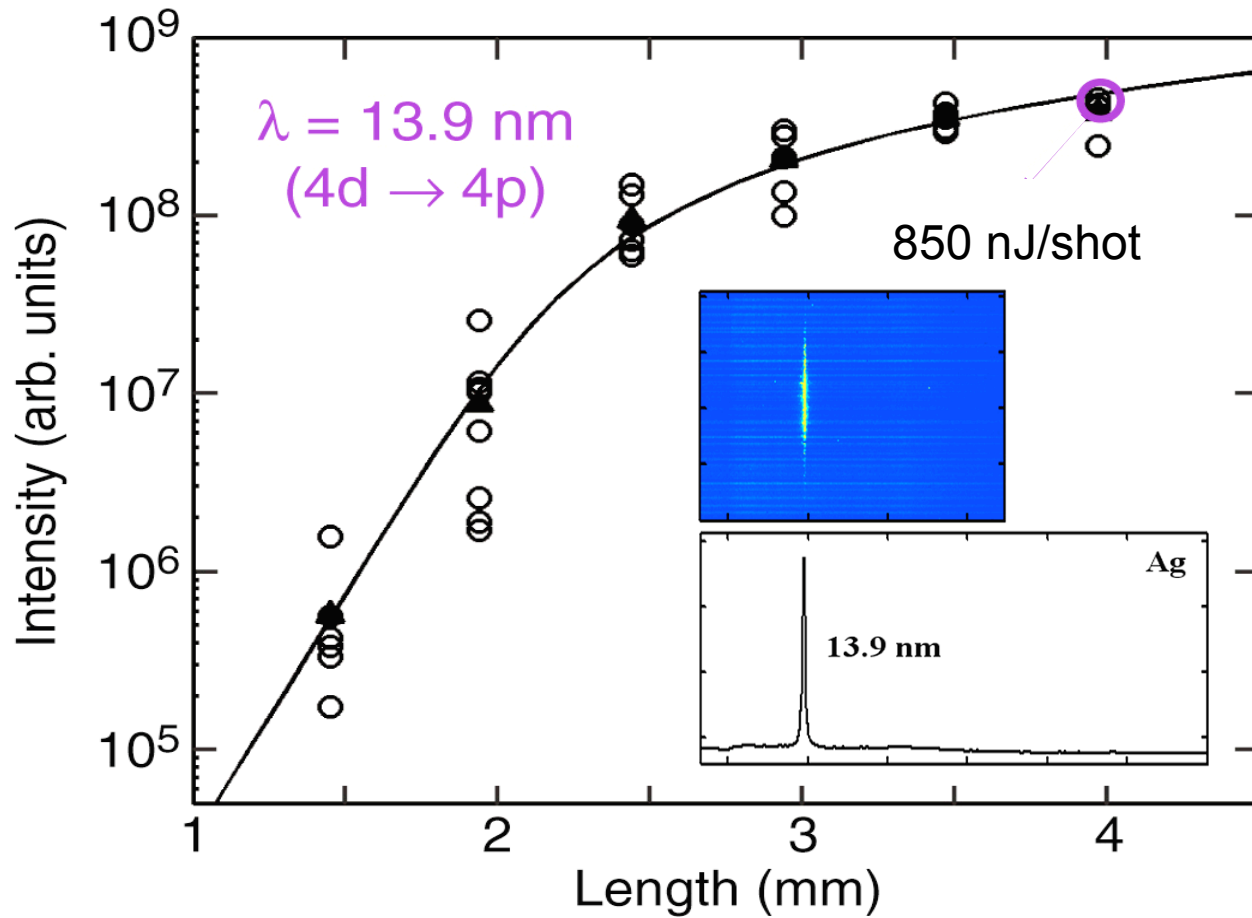


Gain saturated operation demonstrated

Courtesy of J. Rocca
Colo. State U.

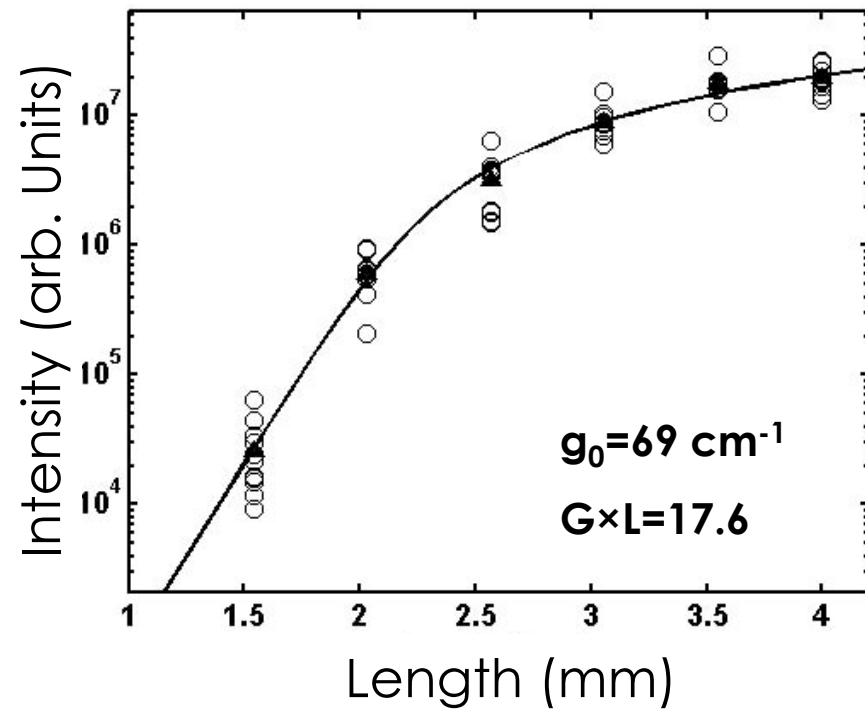
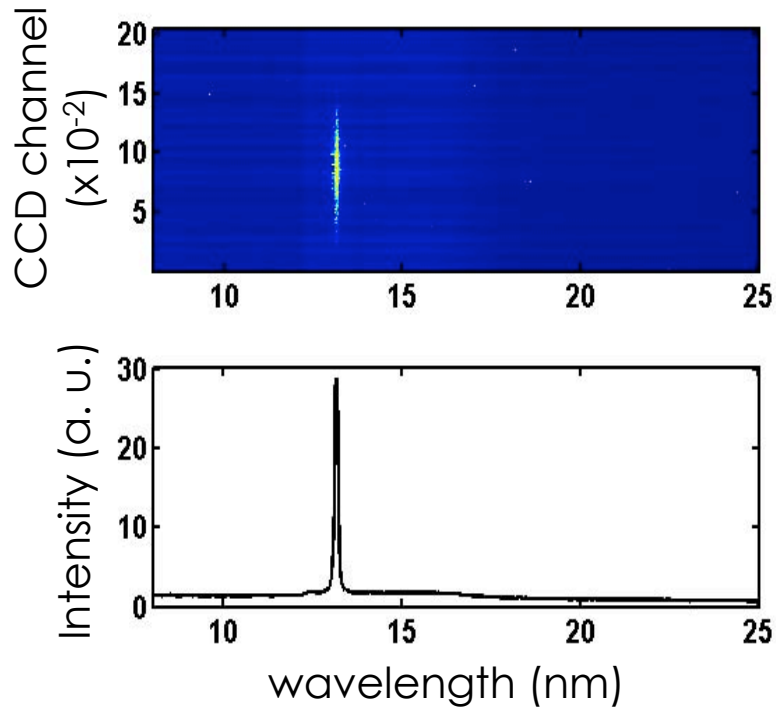
1 J short (8 ps) pulse excitation

$$g_0 = 67 \text{ cm}^{-1}; \quad g_{xl} = 16.8$$



Courtesy of J. Rocca, Colo. State U.

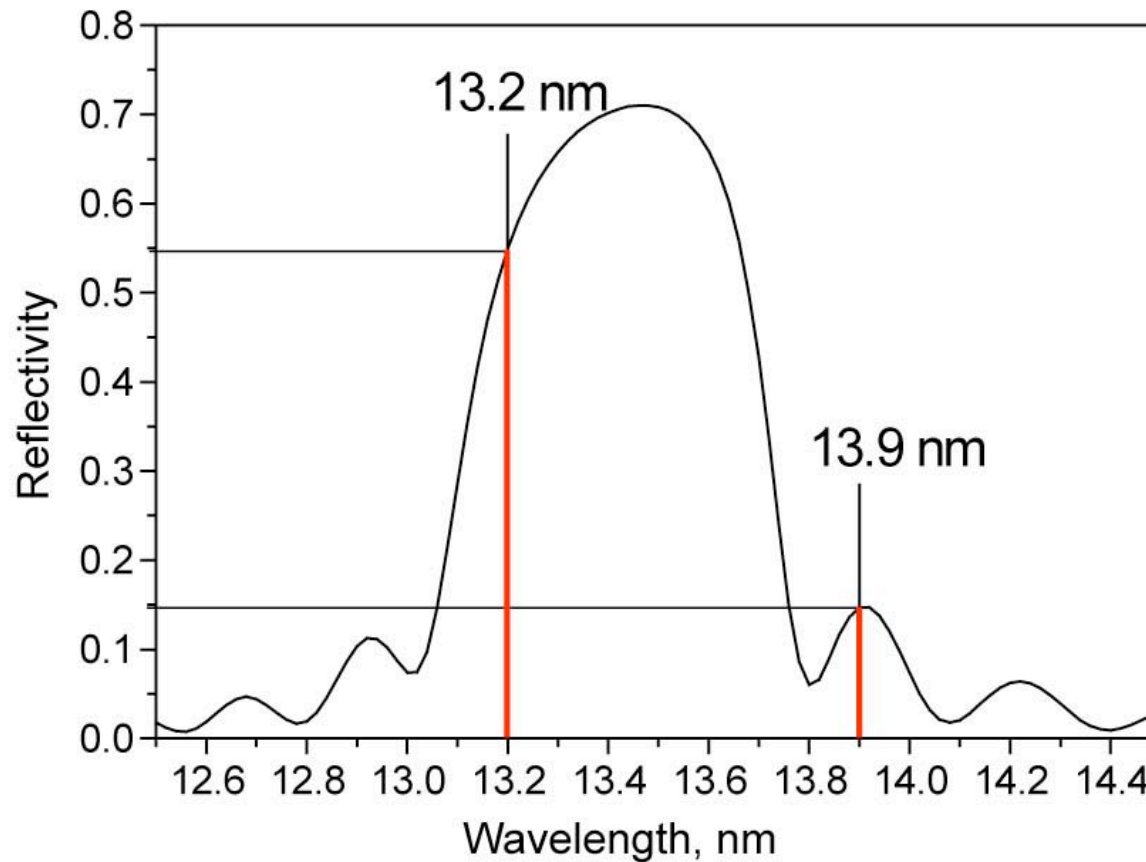
1 J short pulse – 23 degrees grazing incidence angle



Courtesy of J. Rocca, Colo. State U.

A Ni-like Cd at 13.2 nm provides a closer laser wavelength match to Mo/Si lithography mirrors

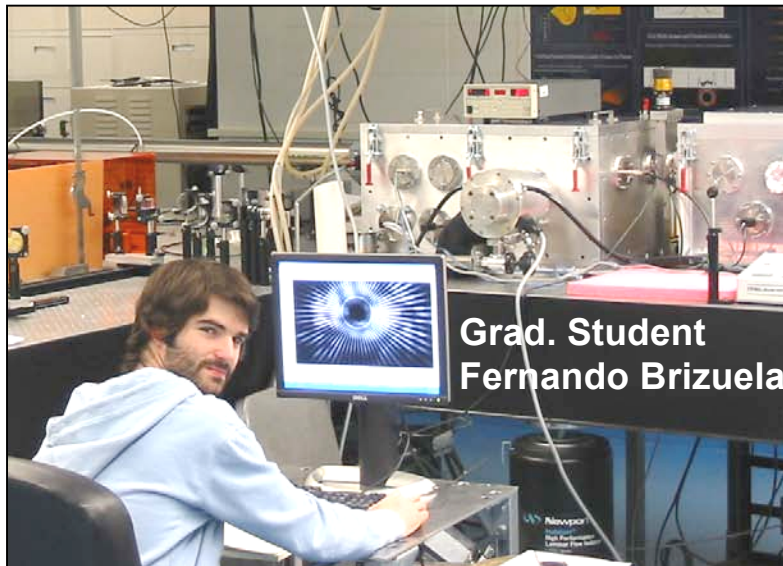
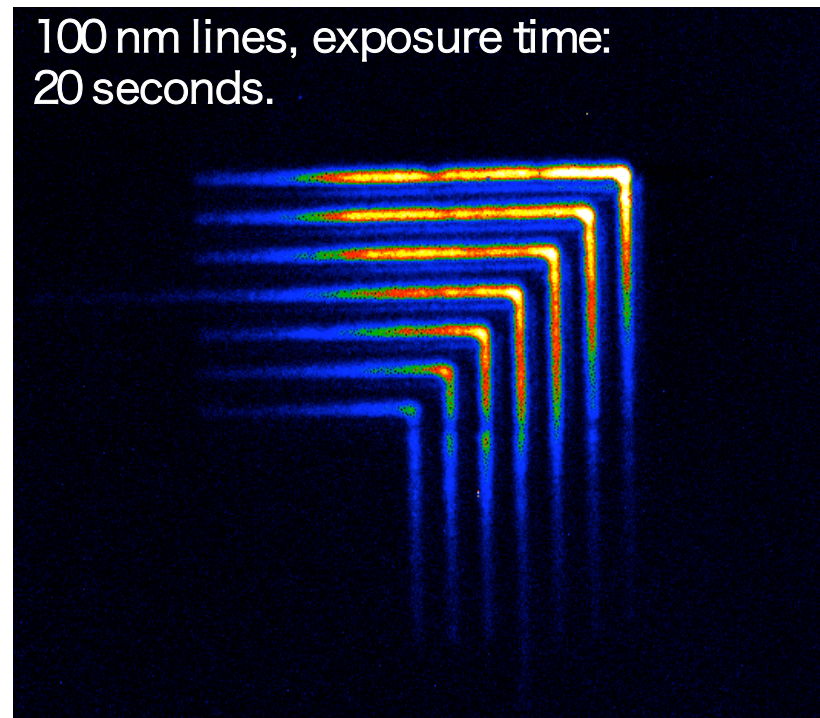
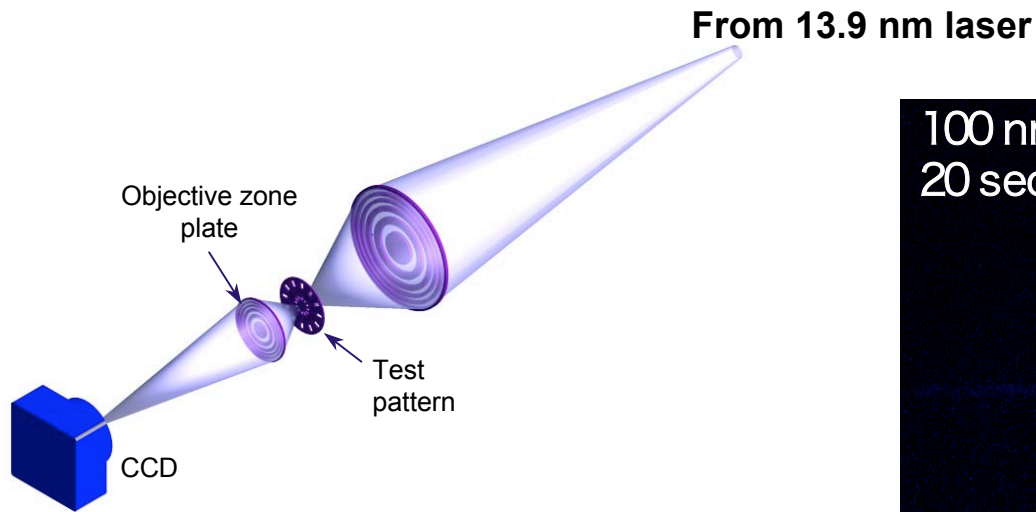
At the wavelength of the Ni-like Cd laser the reflectivity of Mo-Si mirrors centered at $\lambda=13.5$ nm is $\sim 55\%$



Courtesy of J. Rocca, Colo. State U.

The new compact EUV lasers are enabling application testbeds

Example: 13.9 nm Table-top EUV microscope with resolution better than 50 nm



Courtesy of J. Rocca, Colo. State U.